Electrical Wave Filters Employing Quartz Crystals as Elements

By W. P. MASON

This paper discusses the use of piezo-electric crystals as elements in wave filters and shows that very sharp selectivities can be obtained by employing such elements. It is shown that by employing crystals and condensers only, very narrow band filters result. By using coils and transformers in conjuction with crystals and condensers, wide-band-pass and high and low-pass filters can be constructed having very sharp selectivities. The circuit configurations employed are such that the coil dissipation has only the effect of adding a constant loss to the filter characteristic, this loss being independent of the frequency. Experimental curves are given showing the degree of selection possible.

In the appendix, a study is made of the modes of motion of a perpendicularly cut crystal, and it is shown that all the resonances measured can be derived from the elastic constants and the density of the crystal. The effect of one mode of motion on another mode is shown to be governed by the mutual elastic compliances of the crystal. By rotating the angle of cut of the crystal, it is shown that some of the compliances can be made to disappear and a crystal is obtained having practically a single resonant frequency over a wide range of frequencies. Such a crystal is very advantageous for filter purposes.

Introduction

FILTERS for communication systems must pass, without appreciable amplitude distortion, waves with frequencies between certain limits, and must attenuate adequately all waves with somewhat greater or smaller frequencies. To do this efficiently, the change from the filter loss in the transmission region, to that in the attenuation region, must occur in a frequency band which is narrow compared to the useful transmission band. At low frequencies, ordinary electrical coil and condenser filters can perform this separation of frequencies well because the percentage band widths (ratio of band width to the mean frequency of the band) and the percentage separation ranges (ratio of the frequency range required, in order that the filter shall change from its pass region to its attenuated region, to the adjacent limiting frequency of the pass band) are relatively large.

For higher frequency systems, such as radio systems, or high frequency carrier current systems, the band widths remain essentially the same, and hence the percentage band widths become much smaller. Here separation by coil and condenser filters becomes wasteful of frequency space. For these filters, owing to the relatively low reactance-resistance ratio in coils (this ratio is often designated by the letter Q) the insertion loss cannot be made to increase faster than a

certain percentage rate with frequency. Hence an abrupt frequency discrimination cannot be obtained between the passed frequency range and the attenuated frequency range. In present radio systems, double or triple demodulation is often used to supplement the selectivity of filter circuits.

If, however, elements are employed which have large reactance-resistance ratios, filters can be constructed which have small percentage bands and which attenuate in small percentage separation ranges. Such high Q elements are generally obtainable only in mechanically vibrating systems. Of these elements, probably the most easily used is the piezo-electric crystal, for it possesses a natural driving mechanism.

It is the purpose of this paper to describe work which has been done in utilizing these crystals as elements in filters.[1] Since the quartz crystal appears to be the most advantageous piezo-electric crystal, all of the work described in this paper is an application of this type of crystal. The possibilities and limitations are discussed and experimental data are given showing that these filters are realizable in a practical form.

Piezo-electric Crystals and Their Equivalent Electrical Circuits

When an electric force is applied to two plates adjacent to a piezo-electric crystal, a mechanical force is exerted along certain directions which deforms the crystal from its original shape. On the other hand deformations in certain directions in the crystal produce a charge on the electric plates. Hence the crystal is a system in which a mechanical electrical coupling exists between the mechanical and electrical parts of the system.

Quartz crystals, particularly when vibrating along their smallest dimension, as they do for high frequency oscillators, have a large number of resonances which do not differ much in frequency from the principal resonance. While this is no great disadvantage for an oscillator, since an oscillator can pick out the strongest resonance and utilize it only, the large number of resonances is a great disadvantage when using

[1] The development of ideas in the direction of employing crystals as elements of selecting circuits dates back to Cady who in patent—Re. 17,358 issued July 2, 1929, original filed January 28, 1920—showed various types of tuned circuits of which crystals formed a part. Subsequently Espenschied in patent 1,795,204, issued March 3, 1931, filed January 3, 1927—patented broadly the use of crystals as elements of true filter structures. More recently a patent of the writer's—1,921,035 issued August 8, 1933, filed Sept. 30, 1931—describes the use of crystals in lattice structures, and this patent, together with several others pending, forms the basis for the filters discussed in this paper. It is only within the last few years that filter structures including crystal elements have been practically realized.

the crystal to select currents over a wide band of frequencies and to reject currents whose frequencies lie outside this pass region. Hence it is advantageous for filter uses to obtain a crystal which has substantially a single prominent resonance over a wide range of frequencies. Such a vibrating element can usually be obtained only by making the dimension along which the crystal is vibrating, large compared to the other dimensions, and this fact determines the best cut of crystal to use.

Two principal types of orientations have usually been employed in cutting quartz crystals. The first type is the so-called Curie or perpendicular cut in which the crystal is so cut that its major surfaces are parallel to the optical axis and perpendicular to an electrical axis. Such a crystal is shown by Fig. 1. The second type of cut is the parallel

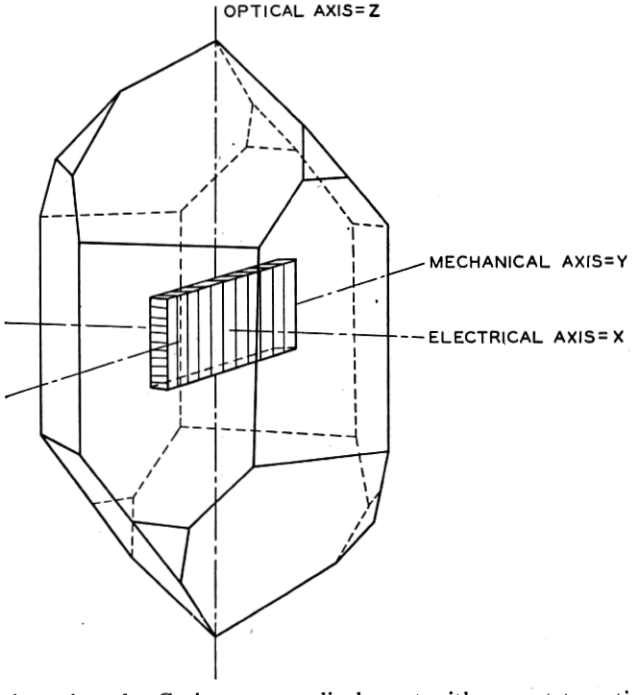

Fig. 1—Orientation of a Curie or perpendicular cut with respect to native crystal.

or 30-degree cut in which the major surfaces of the crystal plate are parallel to both the optical and electrical axes. Since this cut results in a crystal vibrating along its smallest dimension, it is not of much interest for filter uses.

When using a crystal as part of an electrical system, it is desirable

to know the constants of an electrical circuit which has the same impedance characteristic as the crystal. If attention is confined to the single prominent resonance, the electrical circuit representing the crystal is as shown by Fig. 2. Some theoretical consideration has been

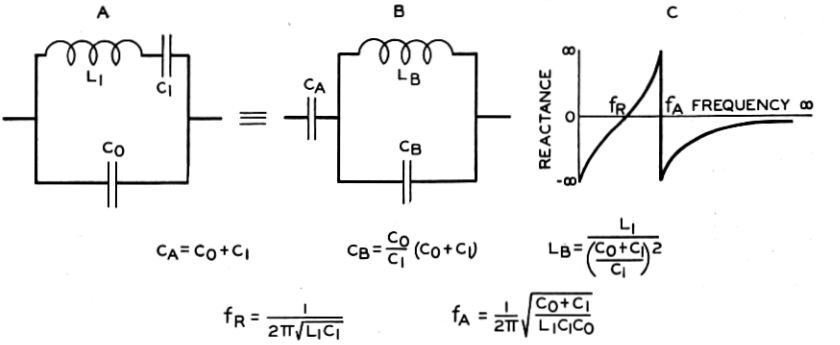

Fig. 2—Equivalent electrical circuit of piezo-electric crystal.

given to the electrical network representing perpendicularly cut crystals by Cady,[2] Van Dyke,[3] Dye,[4] Vigoureux [5] and others. Assuming a quartz plate to have only plane wave motion, Vigoureux has investigated the motion in such a plate, and has shown that there will be resonances at odd harmonics of a particular frequency determined by the length and mechanical constants of the plate. In the neighborhood of the fundamental resonance of the crystal, with the electrical plates placed on the crystal surfaces, he finds the equivalent circuit shown by Fig. 2A, the elements of which in practical units have the following values:

$$C_0 = \frac{l_0 l_m K}{4\pi l_e \times 9 \times 10^{11}} = \text{capacitance in farads},$$

$$C_1 = \frac{l_0 l_m 8 E d_{12}^2}{\pi^2 l_e \times 9 \times 10^{11}} = \text{capacitance in farads}, \qquad (1)$$

$$L_1 = \frac{l_e l_m \rho \times 9 \times 10^{11}}{8 l_0 E^2 d_{12}^2} = \text{inductance in henries},$$

where l_0, l_m, l_e are respectively the lengths of the optical, mechanical, and electrical axes in centimeters,

K = specific inductive capacitance = 4.55 for quartz,
E = Young's modulus = 7.85×10^{11} for quartz,
d_{12} = piezo-electric constant = 6.4×10^{-8} for quartz,
ρ = density = 2.654 for quartz.

[2] W. G. Cady: *Phys. Rev.* XIX, p. 1 (1922); *Proc. I. R. E.* X, p. 83, (1922).
[3] K. S. Van Dyke: Abstract 52, *Phys. Rev.*, June, 1925; Proc. I. R. E., June, 1928.
[4] D. W. Dye: *Proc. Phys. Soc.*, XXXVIII (5), pp. 399–453.
[5] P. Vigoureux: *Phil. Mag.*, Dec., 1928, pp. 1140–53.

Inserting these values, the element values in terms of the dimensions become

$$\begin{aligned} C_0 &= 0.402 \times 10^{-12}\, l_m l_0 / l_e, \\ C_1 &= 0.289 \times 10^{-14}\, l_m l_0 / l_e, \\ L_1 &= 118.2\, l_m l_e / l_0. \end{aligned} \tag{2}$$

From these values it is seen that there is a fixed ratio between these two capacitances [6] of

$$r = C_0/C_1 = 140. \tag{3}$$

As will be evident later, this ratio limits the possibilities of the use of quartz crystals in filter circuits.

Experiments with quartz crystals, with electrodes contiguous to the crystal surfaces and with the optical and electrical axes small compared to the mechanical axis, show that these values are approximately correct. The value of C_0 checks the above theoretical value quite closely. The value of C_1 obtained by experiment is somewhat larger than that given by equation (2) and the value of the inductance somewhat smaller. The ratio of C_0/C_1 has been found as low as 115 to 1, but a value of 125 to 1 is about all that can be realized, when account is taken of the distributed capacitance of the holder, connecting wires, etc.

When either of the dimensions along the electrical or optical axes becomes more than a small fraction of the dimension of the mechanical axis, the plane wave equations given above no longer hold accurately. This is due to the fact that a coupling exists between the motion along the mechanical axis and other modes of motion. For an isotropic body, one is familiar with the fact that when a bar is compressed or stretched it tends to stretch or compress in directions perpendicular to the principal direction of motion. This state of affairs may be described by saying that the modes of motion are coupled. In a crystal this same relation exists and in addition, due to its crystalline form, a shearing motion is set up whose shearing plane is determined by the mechanical and optical axes and whose motion is parallel to the mechanical axis. In fact the shearing motion is more closely coupled to the mechanical axis motion that is the extensional motion. As long as the optical axis is small compared to the mechanical axis, this coupling action manifests itself as a decreased stiffness along the mechanical axis, but if a condition of resonance is approached for the motion along the optical axis, the mode of motion is entirely changed. This effect is

[6] In a paper contributed recently to the *Institute of Radio Engineers*, it is shown that this ratio limitation is a consequence of a fixed electro-mechanical coupling between the electrical and mechanical systems of the crystal.

analyzed in the appendix and is quantitatively explained in terms of the elastic constants of the crystal. On the basis of this explanation, an investigation is also given in the appendix, of crystals cut at different orientations, and a crystal having many advantages for filter uses is derived.

Some experimental data [7] have been taken for perpendicularly cut crystals for various ratios of axes. Figure 3 shows the principal reso-

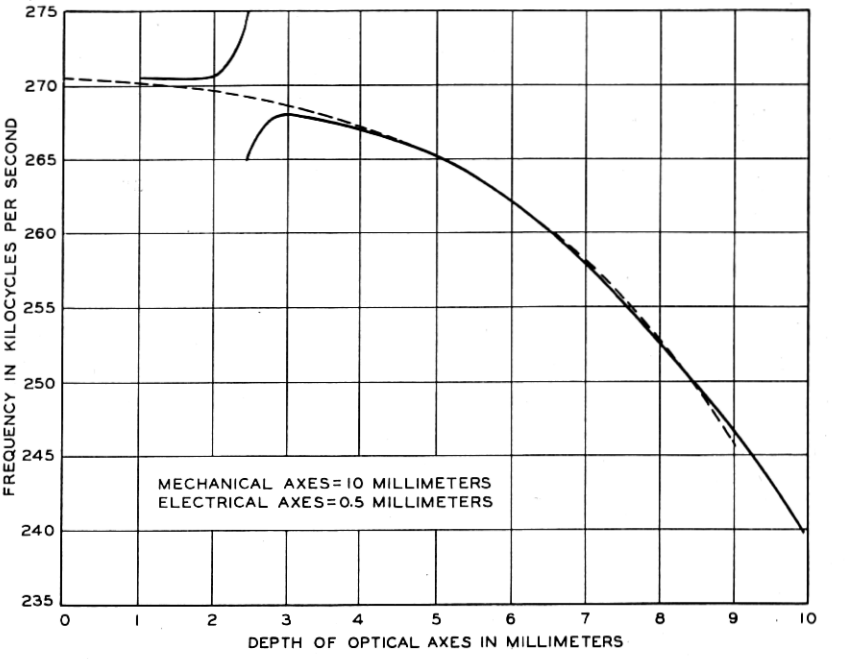

Fig. 3—Principal resonant frequency of a perpendicularly cut crystal as a function of the width of the crystal.

nant frequency (the frequency for which the electrical impedance is a minimum) for a series of crystals whose mechanical axes are all 10 millimeters, whose electrical axes are 0.5 millimeter, and whose optical axes vary from 1 to 10 millimeters. As will be observed, increasing the length of the optical axis in general lowers the resonant frequency. The discontinuity in the curve for the ratio $l_0/l_m = .23$ is discussed in detail in the appendix.

[7] The experimental data shown by Figs. 3 and 4 have been taken by Mr. C. A. Bieling while the temperature coefficient curve of Fig. 5 was measured by Mr. S. C. Hight.

The solid curve of Fig. 4 shows a measurement of the ratio, r, of the capacitances in the simple representation of the crystal shown by Fig. 2A. This ratio is measured by determining the resonant and anti-

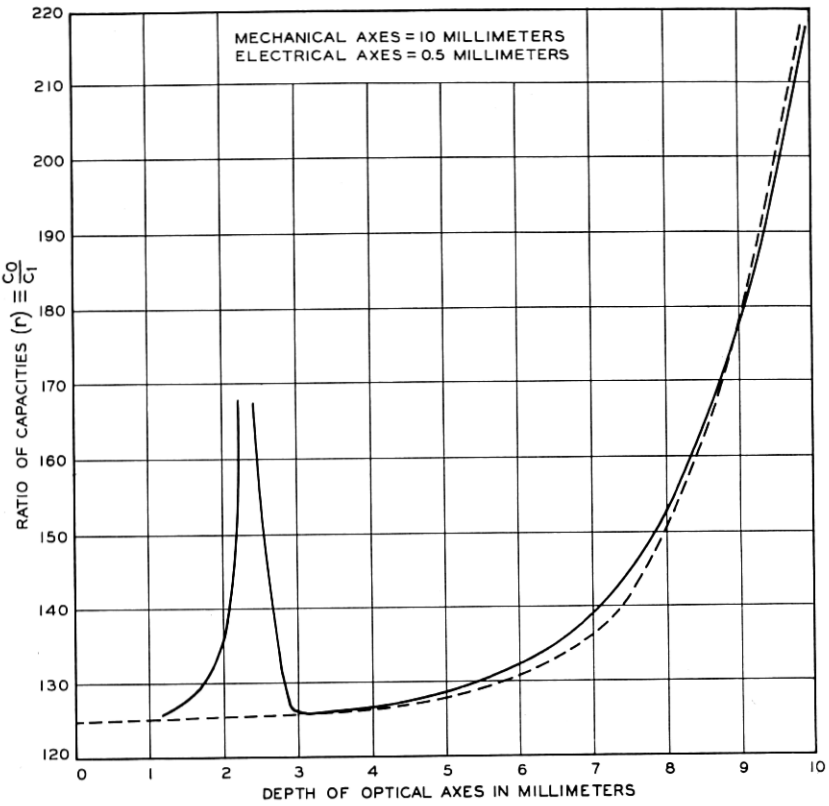

Fig. 4—Ratio of capacitances of a perpendicularly cut crystal.

resonant frequencies of the crystal. r is related to these by the formula

$$f_A^2/f_R^2 = 1 + 1/r, \tag{4}$$

where f_A is the anti-resonant frequency and f_R the resonant frequency.

Figure 5 shows a measurement of the temperature coefficient of the resonant frequency for the same set of crystals. It will be noted that as the optical axis increases in depth, the temperature coefficient increases and that crystals with smaller dimensions along the optical axis in general have much smaller coefficients. Increasing the thickness along the electrical axis has the effect of decreasing the tempera-

ture coefficient and in fact for certain ratios of the three axes the coefficient approaches zero.

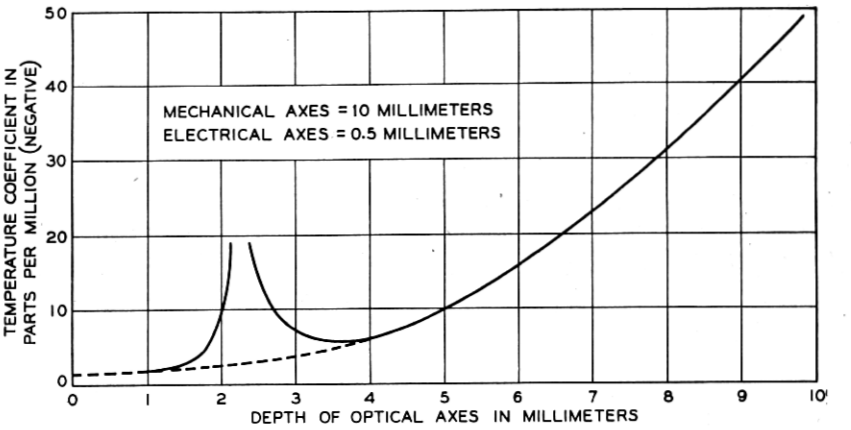

Fig. 5—Temperature coefficient of a perpendicularly cut crystal.

When the crystals are used in filters, two quantities are usually specified, the resonant frequency of the crystal and the capacitance of the series condenser. The shunt capacitance of the crystal is usually incorporated with an electrical capacitance which is specified by other considerations. The resonant frequency is determined principally by the mechanical axis length. The capacitance of the series condenser is determined by the ratio of the area to the thickness or by $l_0 l_m / l_e$. The third condition is given by the fact that the length of the optical axis should be kept as small as possible in order that any subsidiary resonances shall be as far from the principle resonance as possible. The curves of Figs. 3 and 4 and the fact that the resonant frequency of a given shaped crystal varies inversely as the length, can be used to determine the dimensions of the crystal. It is obvious that the crystal should not be used in the region $0.2 < l_0/l_m < 0.3$ on account of the two prominent resonant frequencies.

Use of Crystals and Condensers as Filter Elements

Considering crystals as representable by the simple electrical circuit shown on Fig. 2*A*, these circuits can be utilized as elements in electrical networks. They may, of course, be used in a network employing any kinds of electrical elements. Since, however, their Q is high, it would be advantageous not to employ any electrical elements which do not also have a high Q, in order that the dissipation introduced by these elements may not be a matter of consideration. The

Q's of the best electrical condensers may be as high as 10,000, which is of the same order as the crystal Q, and hence such elements can be employed advantageously with crystals. It is the purpose of this section to discuss the possibilities and limitations of filter sections employing crystals and condensers only.

The simplest types of filter sections are the ladder type networks illustrated by Fig. 6. If crystals and condensers only are employed in

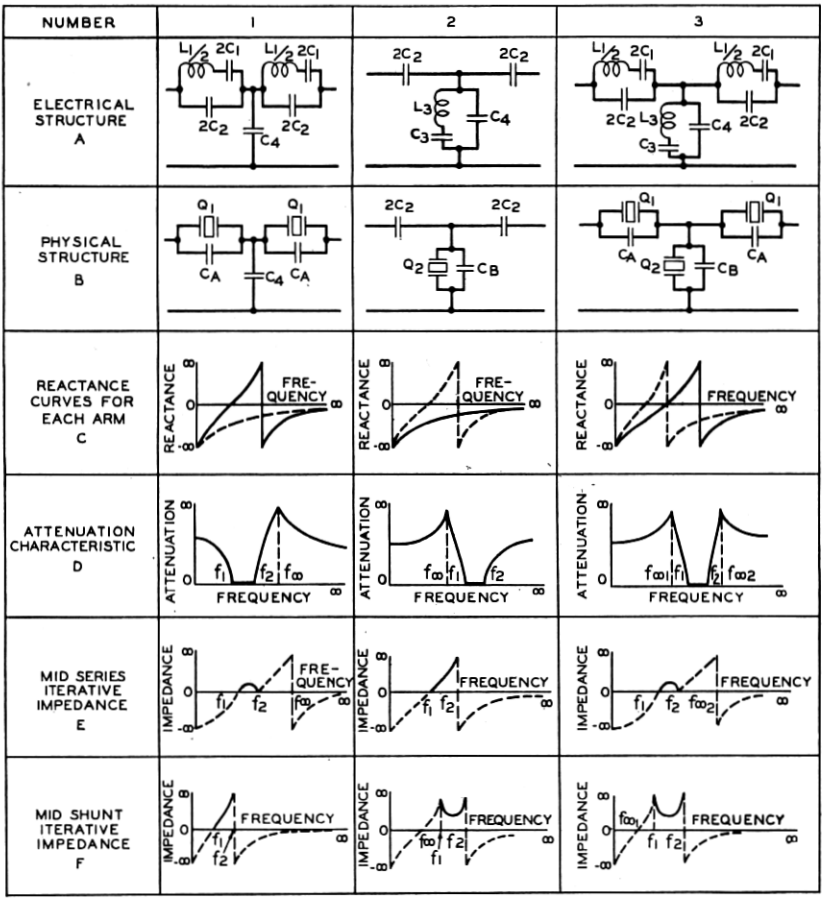

Fig. 6—Ladder networks employing crystals and condensers.

this type network, there are only three types of single band sections possible, all being band-pass filters. Figure 6 shows these sections, the impedance characteristic of each arm, the attenuation characteristics of these networks considered as filters, and their iterative impedances.

These attenuation characteristics and their limitations are at once found from a consideration of the impedance frequency curves for each arm shown by Fig. 6*C*. For a ladder type network it is well known [8] that a pass band will exist when

$$0 \geqq \frac{Z_1}{4Z_2} \geqq -1, \tag{5}$$

where Z_1 is the impedance of the series arm and Z_2 the impedance of the shunt arm. Hence, considering the first filter of Fig. 6, it is obvious that the lower cut-off fc_1 will come at the resonant frequency of the crystal. The upper cut-off fc_2 will come some place between the resonant and anti-resonant frequency, the exact position depending on the amount of capacitance in shunt. The anti-resonant frequency will be a point of infinite attenuation since the filter will have an infinite series impedance at this frequency.

With the restriction on the ratio of capacitances of the crystal noted in the previous section, it is easily shown that the ratio of the anti-resonant frequency to the resonant frequency is fixed and is about 1.004. Hence, we see that the ratio of $f\infty$ to fc_1 can be at most 0.4 per cent. The band width must be less than this since fc_2 must come between $f\infty$ and fc_1. A similar limitation occurs for the second filter of this figure, for which case the separation of $f\infty$ and fc_2 is at most 0.4 per cent. For filter number 3, a somewhat larger frequency separation between the points of infinite attenuation results, it being at most 0.8 per cent. The addition of any electrical capacitance in series or shunt with any of the crystals results in a narrowing of the band width.

It is seen then that there are two limitations in the types of filters obtainable with crystals and condensers in ladder sections. One, there is a limitation on the position of the peak frequencies and two, there is a limitation for the band width of the filters.

By employing the more general lattice type of filter section shown on Fig. 7, the first of these limitations can be removed. By means of this type of section it is possible to locate the attenuation peak frequencies at any position with respect to the pass band, but the pass band is limited in width to at most 0.8 per cent.

For a lattice filter a pass band exists when the impedances of the two arms are related by the expression [9]

$$0 \geqq \frac{Z_1}{Z_2} \geqq -\infty, \tag{6}$$

[8] See, for example, page 190 in book by K. S. Johnson, "Transmission Circuits for Telephonic Communications."

[9] "Physical Theory of the Electric Wave Filter," G. A. Campbell, *B. S. T. J.*, November, 1922.

where Z_1 is the impedance of the series arm (either 1, 2 or 3, 4 of Fig. 7*A*) and Z_2 the impedance of the lattice arm (either 1, 3 or 2, 4 of Fig. 7*A*). Hence, if one pair of branches has a reactance whose sign

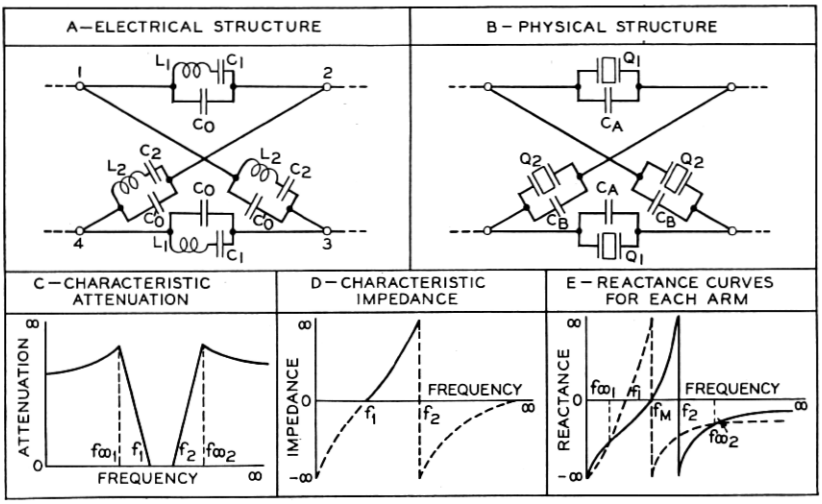

Fig. 7—Lattice network employing crystals and condensers.

is opposite to that of the other pair, a pass band exists, while if they are the same sign an attenuated band exists. Since the lattice is in the form of a Wheatstone bridge an infinite attenuation exists when the bridge is balanced, which occurs when both pairs of arms have the same impedance.

Let us consider a lattice filter with a crystal in each arm as shown by Fig. 7*B*. The crystals form two pairs of identical crystals, two alike in the series arms and two alike in the lattice arms. In order that a single band shall result it is necessary that the anti-resonant frequency of one arm coincide with the resonant frequency of the other as shown by Fig. 7*E*. It is obvious that the band width will be twice the width of the resonant region of the crystal or at most 0.8 per cent. Since the attenuation peaks occur when the two arms have the same impedance, they may be placed in any desired position by varying the impedance of one set of crystals with respect to the other. If crystals alone are used, these peaks will be symmetrical with respect to the pass band, but if in addition condensers are used with these crystals, the peaks may be made to occur dissymmetrically. In fact they may be made to occur so that both are on one side of the pass band. A narrower band results when capacitances are used in addition to crystals since the ratio of capacitances becomes larger. This may be utilized to control the width of the pass band to given any value less than 0.8 per cent.

The use of more crystals than four, in any network configuration employing only quartz crystals and condensers can be shown to result in no wider bands than 0.8 per cent, although higher losses can be obtained by the use of more crystals. Hence by the use of quartz crystals and condensers alone, a limitation in band width to 0.8 per cent is a necessary consequence of the fixed ratio of capacitances C_0/C_1 of equation (3).

Filter Sections Employing Crystals, Condensers and Coils

As was pointed out in the last section, filters employing only crystals and condensers are limited to band pass sections whose band widths do not exceed about 0.8 per cent. This band width is too narrow for a good many applications and hence it is desirable to obtain a filter section allowing wider bands while still maintaining the essential advantages resulting from the use of sharply resonant crystals. Such filters can be obtained only by the use of inductance coils as elements. Since the ratio of reactance to resistance of the best coils mounted in a reasonable space does not exceed 400, attention must be given to the effect of the dissipation.

The effect of dissipation in a filter is two-fold. It may add a constant loss to the insertion loss characteristic of the filter, and it may cause a loss varying with frequency in the transmitting band of the filter. The second effect is much more serious for most systems since an additive loss can be overcome by the use of vacuum tube amplifiers whereas the second effect limits the slope of the insertion loss frequency curve. Hence, if the dissipation in the coils needed to widen the band of the filter has only the effect of increasing the loss equally in the transmitting band and the attenuating band of the filter, a satisfactory result is obtained. The question is to find what configuration the coils must be placed in with respect to the crystals and condensers in order that their dissipation will not cause a loss varying appreciably with frequency.

Not every configuration will give this result, as is shown by the following example. The equivalent circuit of the crystal shown by Fig. 2*A* can be transformed into the form shown by Fig. 8*A* where the ratio $C_1/C_0 = 125$. This gives the same reactance curve as before, limited to a width of 0.4 per cent. Now suppose that we add an electrical anti-resonant circuit in series with the crystal—Fig. 8*B*—resonating at the same frequency and having the same constants as the anti-resonant network representing the crystal. If this circuit were dissipationless we could combine the two resonant circuits into one with twice the inductance and half the capacitance of that for the crystal alone

and hence the capacitance ratio would be 1/2 (125) or 62.5. The band width possible would then be twice that of the crystal alone. However, when the effect of dissipation is considered it is found that not much has been gained by employing the anti-resonant circuit. For the re-

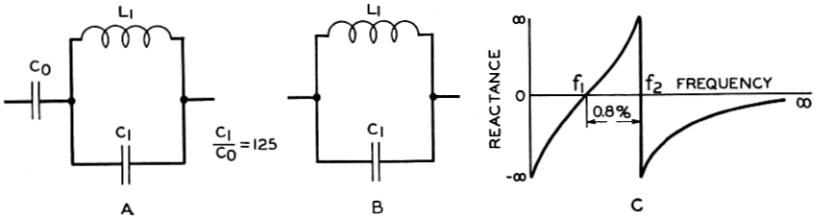

Fig. 8—Use of an anti-resonant circuit to broaden the resonance region of a crystal.

sistance, at resonance of the crystal and electrical circuit combination, will be the resistance of the electrical resonant circuit since that of the crystal is small compared to the electrical element. Hence we have doubled the impedance of the anti-resonant circuit and have the resistance of the electrical circuit. Hence the ratio (Q) of reactance to resistance of the anti-resonant circuit is double that of the electrical element alone. Even this Q, however, is insufficient to make a narrow band filter whose band width is 1.6 per cent (twice that possible with a crystal alone) and hence no useful purpose is served by combining a crystal with an electrical anti-resonant circuit.

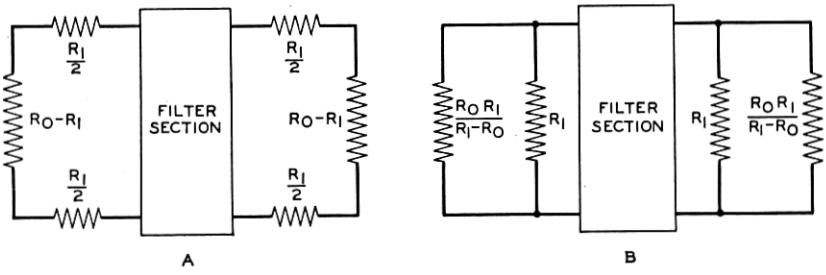

Fig. 9—Circuit showing resistances on the ends of filter sections.

Suppose, however, that all of the dissipation of the filter section be concentrated at the ends of the sections, either in series or in parallel with the filter as shown on Fig. 9. Then provided these resistances are within certain limits, they can be incorporated in the terminal resistances of the filter by making these resistances either smaller or larger for series or shunt filter resistances respectively. Between sections the resistances on the ends of the filter can be incorporated with other

resistances in such a way as to make a constant resistance attenuator of essentially the same impedance as the filter. For a series coil, this can be done by putting a shunt resistance between sections, while for a shunt coil it can be done by putting series resistances between sections. If this is done the whole effect of the dissipation is to add a constant loss to the dissipationless filter characteristic, this loss being independent of the frequency.

Since the lattice type network provides the most general type of filter network, attention will first be directed to this type of section employing inductances. It is easily proved that if any impedance is in series with both sides of a lattice network, as shown by Fig. 10*A*, then

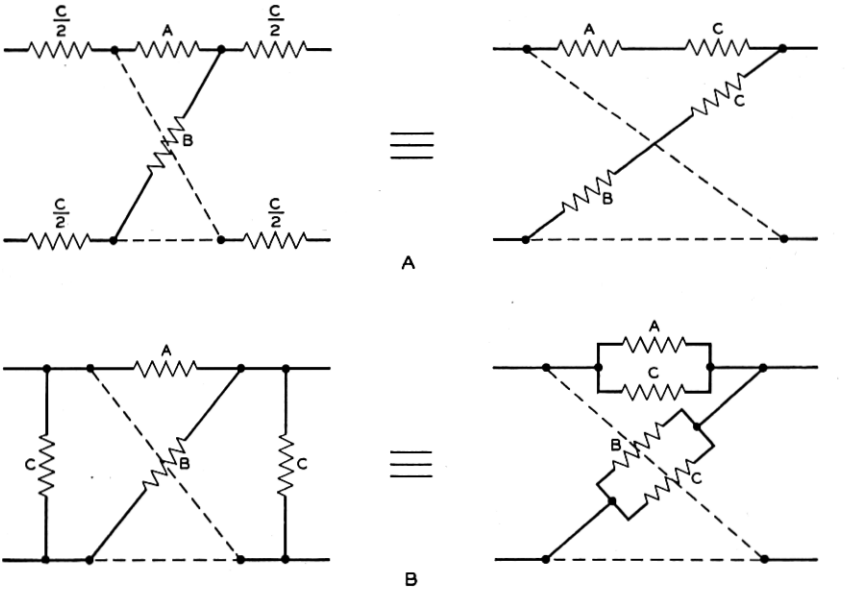

Fig. 10—Two network equivalences.

this is equivalent to placing this impedance in series with each arm of the lattice network as shown. Similarly, if a given impedance shunts the two ends of a lattice network, as shown by Fig. 10*B*, a lattice network equivalent to this is obtained by placing the impedance in shunt with all arms of the lattice. We are then led to consider a lattice network which contains coils either in series or in shunt with the arms of a lattice network, these arms containing only crystals and condensers, since the dissipation will then be effectively either in series or in shunt with the lattice network section.

If an inductance is added in series with a crystal the resulting re-

actance is shown by the full line of Fig. 11; the dotted lines show the reactance curves for the individual elements. It is evident that the resonant frequency of the crystal is lowered, the anti-resonant point remains the same, and an additional resonance is added at a frequency

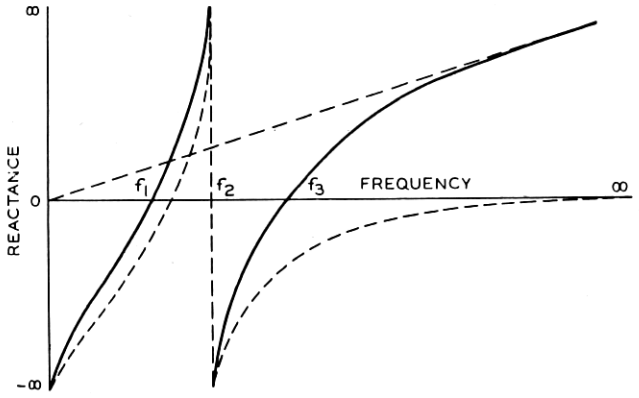

Fig. 11—Impedance characteristic of crystal and coil in series.

above the anti-resonant frequency. For a crystal whose ratio of capacitances r is about 125 it is easily shown by calculation that if the resonances are evenly spaced on either side of the anti-resonant frequency the percentage frequency separation between the upper resonance and the lower resonance is in the order of 9 per cent.

Suppose now that this element is placed in the series arm of a lattice network and another element of similar character is placed in the lattice arm, the second element having its lowest resonance coincide with the anti-resonance of the first element, and having the anti-resonance of the second element coincide with the highest resonance of the first element. This condition is shown by Fig. 12*C*. This network will produce a band-pass filter whose band extends from the lowest resonance of the series arm to the highest resonance of the lattice arm, a total percentage frequency band width of 13.5 per cent. By designing the impedances correctly the impedances of the two arms can be made to coincide three times so that there is a possibility of three attenuation peaks due to this section as shown by Fig. 12*D*. The loss introduced by the filter is equivalent to that introduced by three simple band-pass sections. Ordinarily the coils in the two arms are made equal so that their resistances are equal and for this case one of the peaks occurs at an infinite frequency. Since the resistances are equal, then by the theorem illustrated by Fig. 10*A* these resistances can be brought out on the ends and incorporated with the terminal

resistances, with the result that the dissipation of the coils needed to broaden the band has only the effect of adding a constant loss to the filter characteristic, this loss being independent of the frequency.

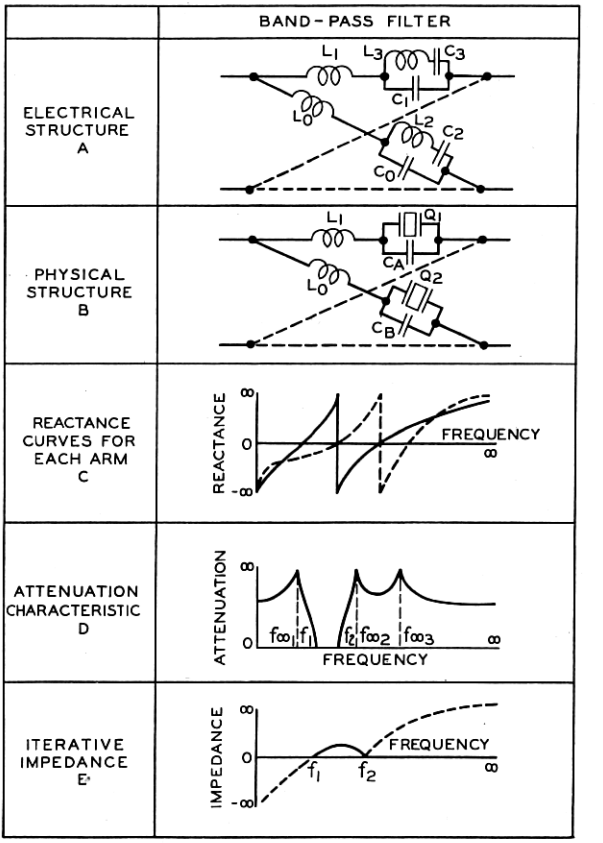

Fig. 12—Lattice network band-pass filter employing series coils.

To vary the width of the band below the 13.5 per cent band obtained with crystals only, added capacitances can be placed in parallel with the crystals increasing the ratio r. This results in a smaller separation in the resonant frequencies and hence a narrower band width. By this means the band width can be decreased indefinitely, although the dissipation caused by the coils introduces large losses for band widths much less than 1/2 per cent. By this means, however, it is possible to obtain band widths down to the widths which can be realized with crystals alone. On the upper side electrical filters can be built whose widths are as small as 13.5 per cent, hence this method fills

in a range not practical with electrical filters, or with crystals alone.

Another important characteristic of the filter is its iterative impedance. For a lattice filter this is given by [9]

$$Z_I = \sqrt{Z_1 Z_2},$$

where Z_1 is the impedance of the series arm and Z_2 that of the lattice arm. For a dissipationless filter, this is shown by Fig. 12*E*, as can be easily verified by a consideration of the reactance curves of Fig. 12*C*.

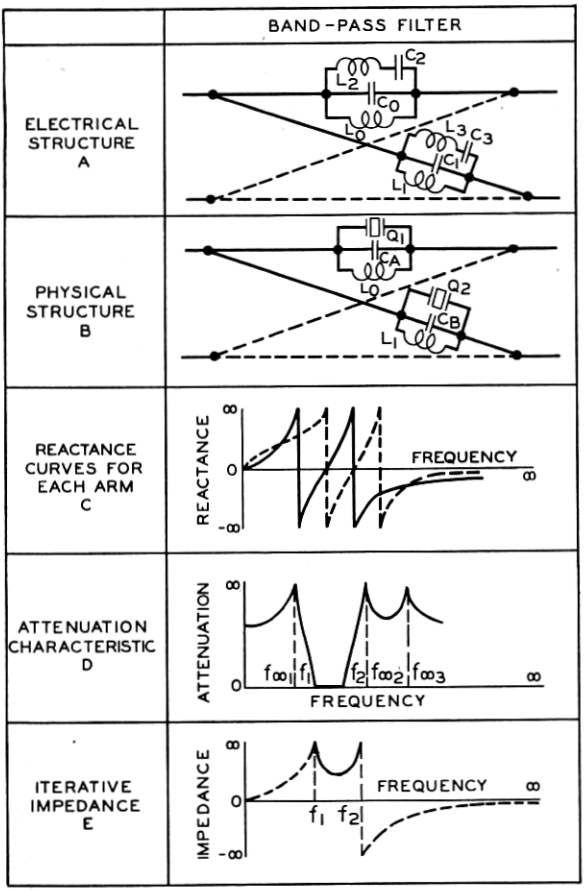

Fig. 13—Lattice network band-pass filter employing parallel coils.

This type of filter results in a relatively low impedance, for example about 600 ohms for a filter whose mid-band frequency is 64 kilocycles and whose band width is that shown on Fig. 19. Since the band width is decreased by adding more capacitance, it is evident that smaller

percentage band width filters will have lower impedances than the wider ones. For example, the filter whose characteristic is shown by Fig. 20, has an iterative impedance of 25 ohms.

It is evident that a still wider band can be obtained with the section discussed above by making the two resonances of Fig. 11 dissymmetrical. If the lower one is brought in closer to the anti-resonant frequency the top one extends farther out in such a manner that the total percentage frequency separation is greater than 9 per cent. If one element of this type is combined with one whose lower resonance is brought farther away from the anti-resonance than is the upper resonance, a filter whose pass band is greater than 13.5 per cent is readily obtained. On the other hand as the band is widened by this means, the cross-over points of the impedances of the two arms are of necessity brought very close to the cut-off frequencies, so that such a filter would introduce most of its loss very close to the cut-off frequencies. This type of characteristic might be useful in supplementing the loss characteristic possible with electrical elements, but by itself would not produce a very useful result.

We have so far discussed the characteristics which can be obtained by placing coils in series with crystals. An equally useful result is obtained by placing coils in shunt with crystals as shown by Fig. 13*B*. This arrangement results in a band-pass filter capable of giving the same band width as the first type discussed above. The only difference

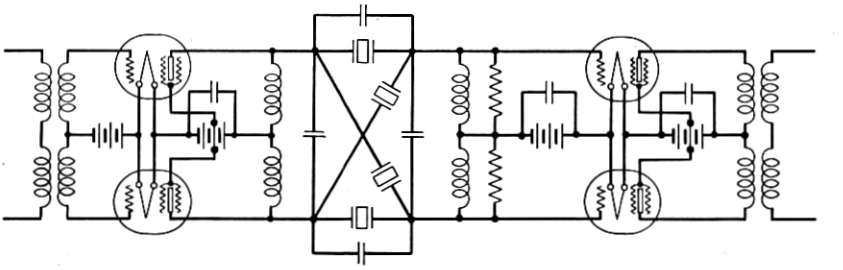

Fig. 14—Band-pass filter used between vacuum tubes.

occurs in the iterative impedance which will be as shown by Fig. 13*E*. For narrow band widths this type of filter has a very high iterative impedance. For example, for a one per cent band width, using ordinary sized coils and crystals, the iterative impedance may be as high as 400,000 ohms. Such filters can be used advantageously in coupling together high impedance screen gird tubes without the use of transformers. One such circuit is shown schematically by Fig. 14.

Filters made by using either series or shunt coils in conjunction

with condensers and crystals make very acceptable band-pass filters capable of moderate band widths. It is often desirable to obtain low and high-pass filters having a very sharp selectivity. The filter of Fig. 12 can be modified to give a high-pass characteristic by leaving out the coils in the series or lattice arms of the network. However, it will be found that the cross-over points in the impedance curve of necessity come very close to the pass band and hence no appreciable loss can be maintained at frequencies remote from the pass band. A broader and more useful characteristic is obtained by using a transformer having a preassigned coefficient of coupling, in conjunction with crystals and condensers, as the element for broadening the separation of resonances. Such an element is shown by Fig. 15*A*. As is well known, a trans-

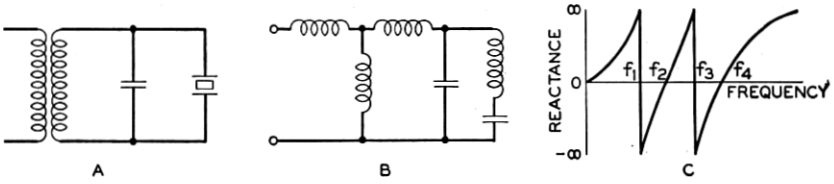

Fig. 15—Impedance characteristic of a transformer, condenser, and crystal.

former with a specified coupling can be replaced by a T network of three inductances as shown by Fig. 15*B*. The impedance characteristic, as shown by Fig. 15*C*, has two anti-resonant frequencies f_1 and f_3, and two resonant frequencies f_2 and f_4.

Suppose now that an element of this type is placed in one arm of the lattice and a similar element having a condenser in series with it is placed in the other arm as shown by Fig. 16*A*. If the elements are so proportioned that the anti-resonances of one arm coincide with the resonances of the other arm and vice versa, as shown by Fig. 16*B*, the impedances of the two arms are of opposite sign till the last resonance. Hence, a low pass filter results. It is possible to make the two impedance curves cross five times, so that an attenuation corresponding to five simple sections of low-pass filter results. Other arrangements of the resonances are also possible and are advantageous for special purposes. For example, as shown by Fig. 16*C*, we can make the last resonance and anti-resonance of both arms coincide, and the other resonances of one arm coincide with the anti-resonances of the second arm. This arrangement results in a low-pass filter having an attenuation corresponding to three simple low-pass filter sections and an impedance which can be made nearly constant to a frequency very near the cut-off frequency. This is advantageous for obtaining a filter with

a sharp cut-off, for otherwise the mismatch of impedance near the cut-off frequency causes large reflection losses which prevent the possibility of obtaining a sharp discrimination.

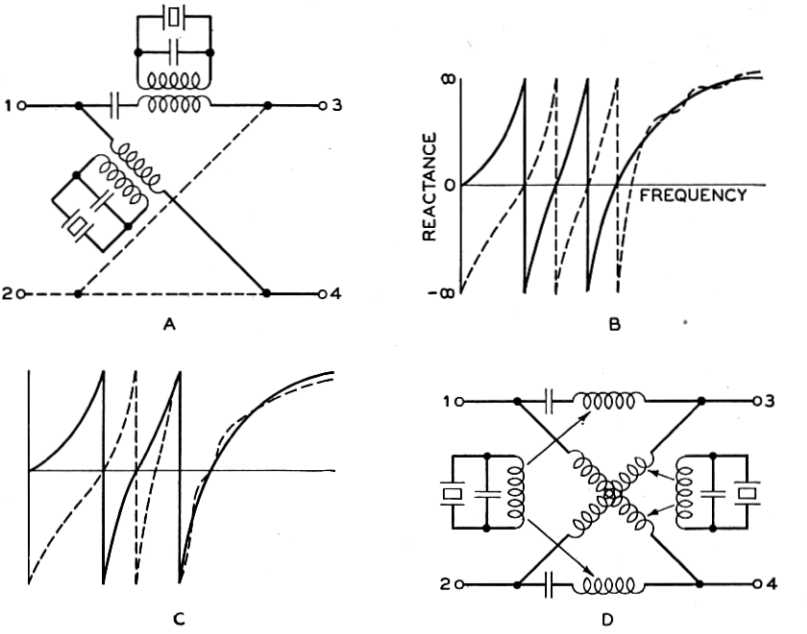

Fig. 16—Lattice network low-pass filter employing transformers, condensers, and crystals.

The effect of dissipation in the transformer on the loss characteristic is not so easy to analyze in this case as in the case of a series coil. The effect can be obtained approximately as follows. Of the three coils of Fig. 15*B* representing the transformer, the shunt coil has the least dissipation since no copper losses are included in this coil. For an air core coil, the Q of this shunt coil becomes very high and its dissipation can be neglected. The resistance of the primary winding can be incorporated in the terminal resistance as in the series coil type of filter and hence will cause only an added loss. The resistance of the secondary will be in series with the crystal and condenser, and for a reasonably good coil is of the same order of magnitude as the crystal resistance at resonance. Hence its effect will be much the same as cutting the Q of the crystal in half, so that instead of a crystal whose Q is 10,000, we use one whose Q is 5000 and a dissipationless coil. We see then that the Q of the crystal is still the most important factor in determining the sharpness of cut-off in the filter as in the previous

ones described, and hence a very sharp selectivity can be obtained with this circuit. It is possible to save elements in this filter by using two primaries for each coil, putting one primary in one series or lattice arm and the other in the corresponding series or lattice arms as shown by Fig. 16*D*. Only half the number of elements per section are required.

By replacing the series condenser of the series arm of Fig. 16*A* by a parallel condenser, it is possible to change the filter from a low-pass to a high-pass filter. Condensers in series, or in parallel with both arms result in wide band-pass filters. It is possible to obtain a wider pass band with this type of filter than with the single coil type since the resonances will be spread over a wider range of frequencies.

In a good many cases it is desirable to have unbalanced filter sections rather than the balanced type which results from the use of a lattice network. This is particularly true for high impedance circuits for use with vacuum tubes. Since the lattice type section is the most general type, it gives the most general characteristics obtainable. The filter sections described here can in some cases be reduced to unbalanced bridge T sections by well known network transformations, with, however, more restrictions on the type of attenuation characteristics physically obtainable.

A very simple bridge T network, which is equivalent to a lattice network of the kind shown on Fig. 13, with two crystals replaced by condensers, is shown on Fig. 17. This section employs mutual induct-

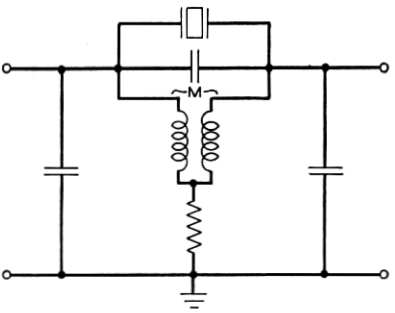

Fig. 17—Single crystal bridge T band-pass filter.

ance, and the resistance [10] shown is necessary in order to balance the arms of the equivalent lattice. This type of network is able to reproduce some of the characteristics of the lattice filter, but is not so general and is, moreover, affected by the dissipation of the coil to a larger extent than the equivalent lattice.

[10] The use of this resistance was suggested by Mr. S. Darlington and practically all the work of developing this filter has been done by Mr. R. A. Sykes.

Experimental Results

A number of filters have been constructed, during the past four years, which employ quartz crystals as elements. Figure 18 shows the measured insertion loss characteristic of a narrow band filter [11] employ-

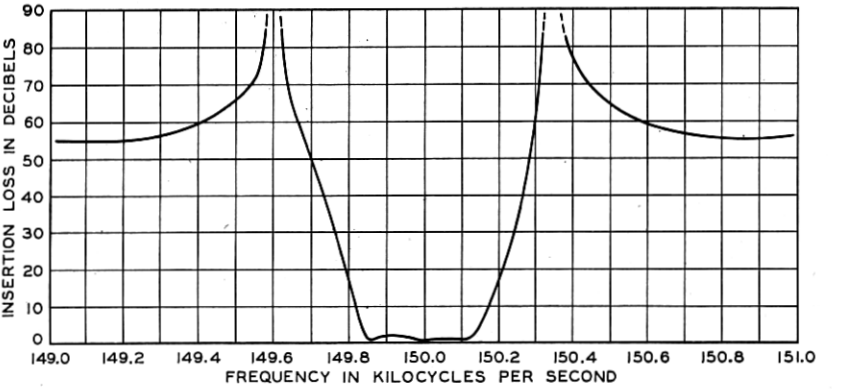

Fig. 18—Measured insertion loss characteristic of a narrow band-pass filter.

ing only crystals and condensers. This filter employs two sections of filter No. 3 of Fig. 6. It will be noted that in spite of the very narrow band width, the insertion loss in the transmitted band is quite small.

A number of the broader band filters employing coils as well as condensers and crystals have also been constructed. The frequency range so far developed extends from 36 kilocycles to 1200 kilocycles. Figure 19 shows the insertion loss characteristic of a band-pass filter whose mid-frequency is 64 kilocycles and whose band width is 2500 cycles. The insertion loss rises to 75 db, 1500 cycles on either side of the pass region. This filter was constructed from two sections of the band-pass type described in Fig. 12. A similar insertion loss characteristic, but shifted to a higher frequency, is shown by Fig. 20. The insertion loss in the center of the band for this higher frequency filter is considerably larger due to the smaller percentage band width. It is interesting to note that practically all of this loss is due to the dissipation introduced by the coils. The useful percentage band width is about one-half per cent and the filter reaches its maximum attenuation

[11] The filters whose characteristics are shown on Figs. 18 and 21 were designed and constructed by Messrs. C. E. Lane and W. G. Laskey. The author wishes to call attention to the fact that they and others associated with them in the Laboratories have made considerable progress in connection with the practical difficulties encountered in the design and construction of these filters such as working out the high precision element adjustment methods required, in methods of mounting, and in shielding methods.

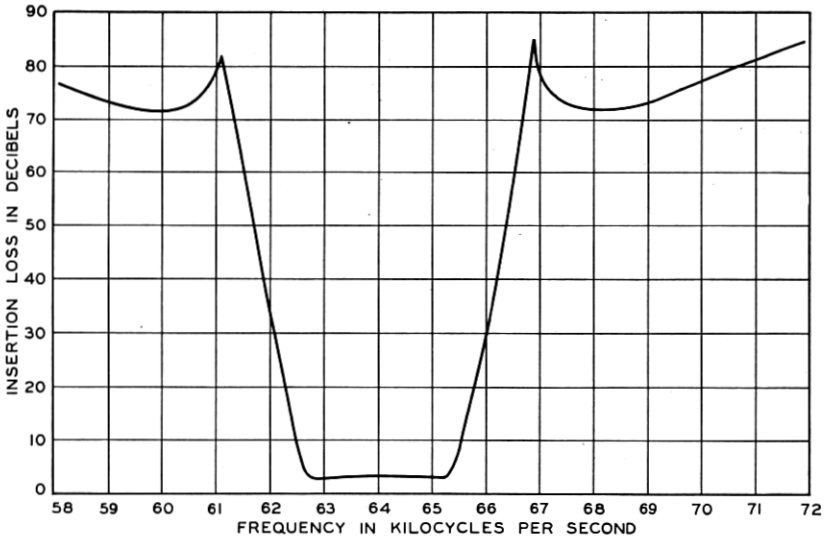

Fig. 19—Measured insertion loss characteristic of a band-pass filter.

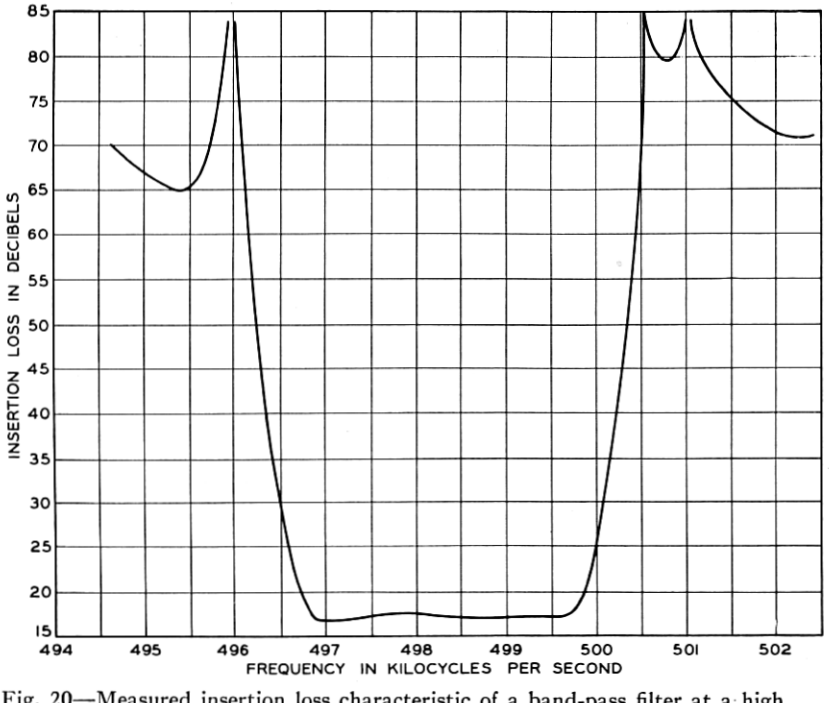

Fig. 20—Measured insertion loss characteristic of a band-pass filter at a high frequency.

in less than one-fourth per cent frequency range on either side of the pass band.

Figure 21 shows the insertion loss characteristics of a filter employed

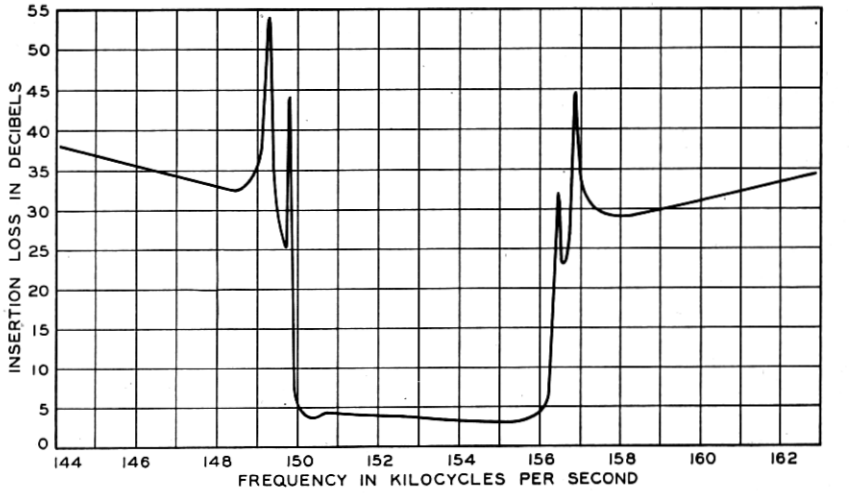

Fig. 21—Measured insertion loss characteristic of a band-pass filter used in a single side band radio receiver.

in an experimental radio system for separating the two sidebands of a channel at a high frequency. Here the separation is effected in about 0.15 per cent frequency range. With the best electrical filters the frequency space required for such a separation is about 1.5 per cent.

Figure 22 shows the insertion loss characteristic of a high-pass filter

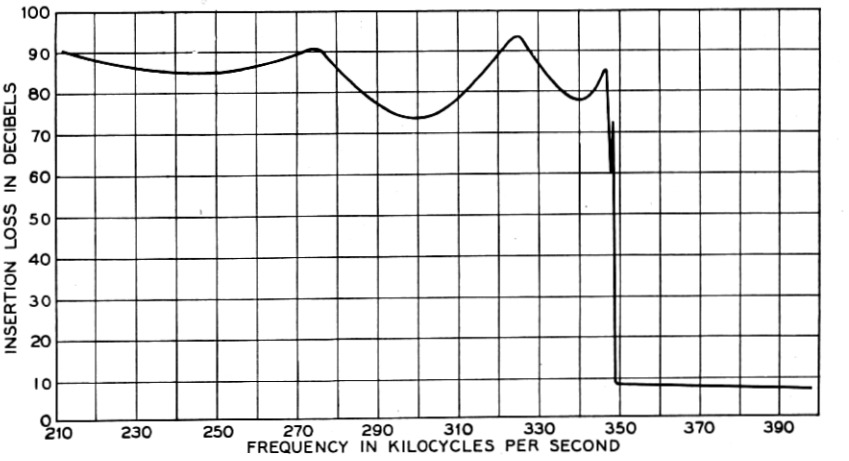

Fig. 22—Measured insertion loss characteristic of a high-pass filter.

constructed by using the circuit of Fig. 16*D*, modified by using a parallel condenser rather than a series condenser. The filter obtains a 65 db discrimination in less than a 0.12 per cent frequency separation.

Figure 23 shows a characteristic obtained by employing a filter of

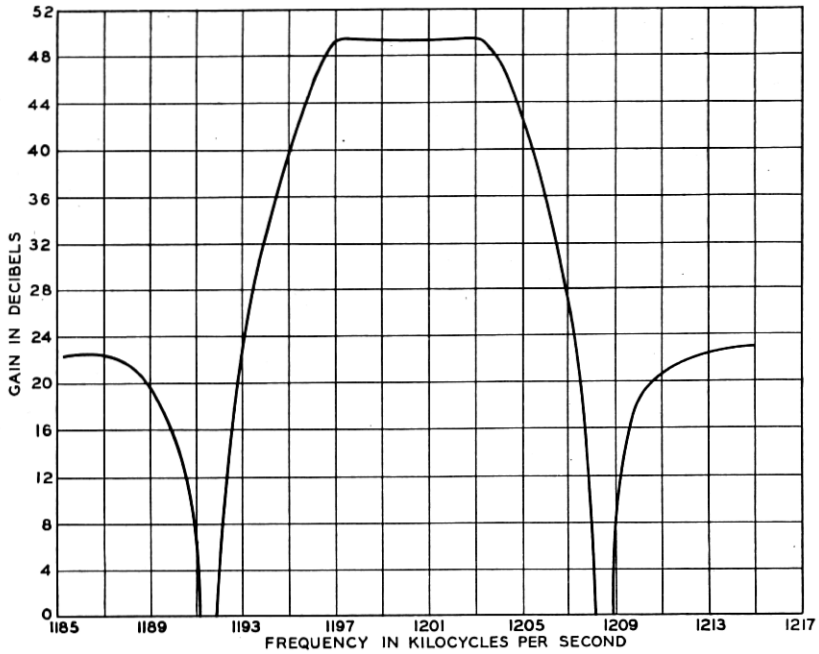

Fig. 23—Measured insertion loss characteristic of a single crystal bridge T filter.

the type shown by Fig. 17, together with a screen grid vacuum tube. The result is plotted as the gain of the circuit since this gives the most significant result for this type of circuit.

APPENDIX

The Modes of Vibration of a Perpendicularly Cut Quartz Crystal

Introduction

Quartz crystals have been cut into two principal types of orientations with respect to the natural crystal faces. The first type is the so-called Curie or perpendicular cut in which the crystal is so cut that its major surfaces are perpendicular to an electrical axis and parallel to the optical axis. Figure 1 shows such a cut. The second type is the so-called parallel or 30-degree cut in which the major surfaces are parallel

to both the optical and electrical axes. In this appendix a study is made of the modes of motion of a perpendicularly cut crystal. The effect has been studied of rotating the direction of the principal axis while still maintaining the principal surfaces perpendicular to the electrical axis. Such a crystal is designated as a perpendicularly cut crystal with an angle of rotation θ.

The perpendicularly cut crystal has received considerable theoretical and experimental consideration especially from Cady,[2] Van Dyke,[3] Dye [4] and Vigoreux.[5] They have assumed that the crystal has a plane wave vibration, and have calculated the frequencies of resonance in terms of the elastic constants and the density of the crystal, and have derived equivalent electrical networks for giving their electrical impedance. Such representations indicate that there should be one resonance for the crystal, the frequency of which is inversely proportional to the length and independent of the width of the crystal. As long as the length of the mechanical axis is large compared to that of any other axis, this prediction agrees with the experiment, but when the length of the other axes become comparable with that of the mechanical axis, the prediction is no longer fulfilled by experiment. It has long been recognized that this deviation is due to the failure of the plane wave assumption. Rayleigh [12] has given a correction for taking account of lateral motion, which is applicable to an isotropic medium. In a crystal, shear vibrations may be set up as well and for this case Rayleigh's correction can only be regarded as qualitative. Also if the other sets of resonance frequencies are to be investigated, account must be taken of the resonances of the other modes of vibration, and their reaction on the mode to be studied.

In this appendix experimental results have been obtained showing the frequencies of resonance found in perpendicularly cut crystals of various shapes and orientations. These frequencies are correlated with the elastic constants of the crystal and are shown to be completely accounted for by them. A coupled circuit representation is developed which is capable of predicting the main features of the principal vibration, including the change of frequency with the shape and orientation of the crystal, and the temperature coefficient curves.

Experimental Determination of the Resonant Frequencies

In order to investigate the modes of motion in a perpendicularly cut crystal in which the main axis coincides with the mechanical axis of the crystal, a set of measurements has been made on crystals whose

[2, 3, 4, 5] Loc. cit.

[12] Rayleigh, "Theory of Sound," Vol. I, Chapter VII, page 252.

mechanical axes are all 1.00 centimeter long, whose electrical axes are very thin, being 0.05 centimeter, and whose optical axes vary in dimension from 0.1 centimeter to 1.00 centimeter. In order to eliminate the effect of a series capacitance due to an air gap, the crystals were plated with a very thin coat of platinum. The effect of an added shunt capacitance in parallel with the crystal, due to the electrode capacitances, was practically eliminated by running the crystal electrodes in an outer grounded conductor as shown in Fig. 24, which shows the

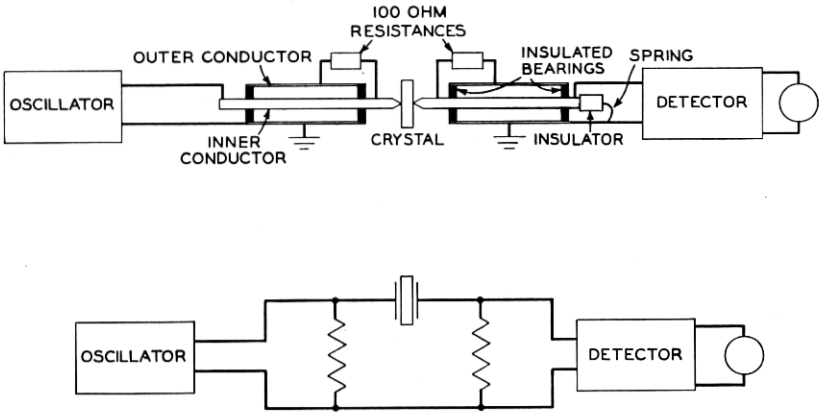

Fig. 24—Measuring circuit used to measure the resonances of a crystal.

measuring circuit. Contact to the crystal plating is made by means of small electrode points placed at the center of the crystal and kept in place by a small pressure. An increase in pressure over a moderate range was found to have no effect on the frequency of the crystal. The lowering of frequency due to plating was evaluated by depositing several films of known weight on the crystal and plotting its resonant frequency as a function of film weight. The intercept of this curve for a zero plating was taken as the frequency of the unplated crystal.

When the frequency of the oscillator was varied, the current in the detector showed frequencies of maximum and minimum current output which are respectively the frequencies of resonance and anti-resonance of the crystal. In order to locate accurately the frequencies of anti-resonance, it was found necessary to insert a stage of tuning in the detector, in order to discriminate against the harmonics of the oscillator. For a given crystal the frequency of the oscillator was varied over a wide range and the resonant and anti-resonant frequencies of the crystal were measured. The results of these measurements are shown by Fig. 25. In this curve the bottom part of the line repre-

sents the actual measured frequency, while the width of the line is proportional to the frequency difference between resonance and anti-resonance. In order to make this quantity observable, the frequency difference between resonance and anti-resonance is multiplied by a factor 6.

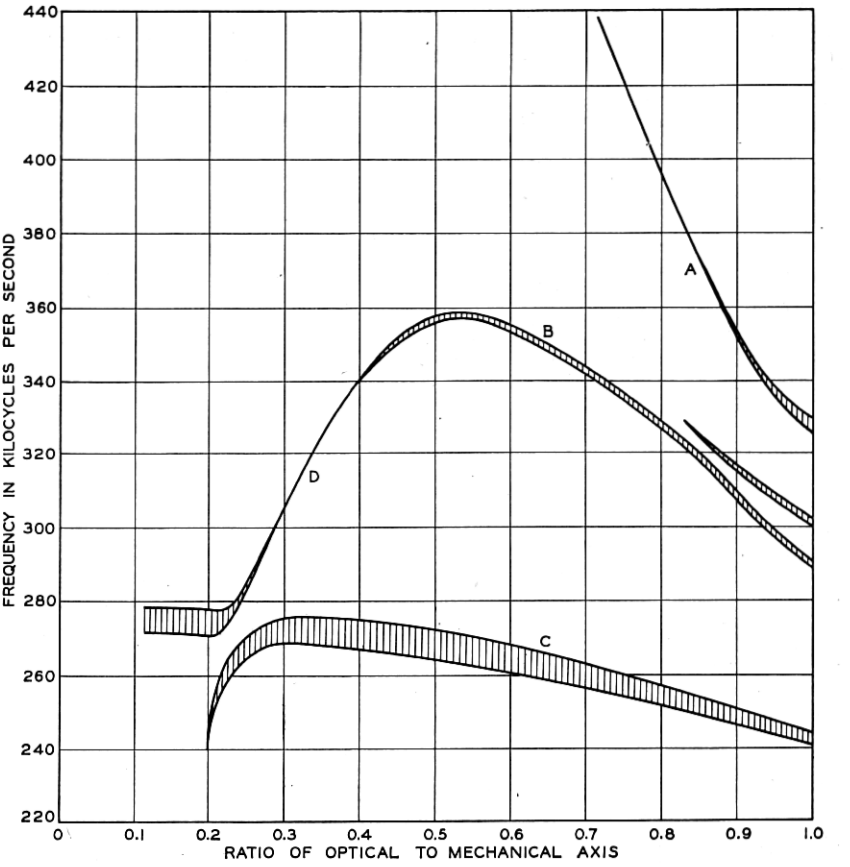

Fig. 25—Measured resonances of a perpendicularly cut crystal.

As long as the ratio of the optical to the mechanical axis is less than 0.2, the assumption of plane wave motion agrees well with experiment since there is only one resonance and its frequency does not depend to any great extent on the optical axis. However, above this point two frequencies make their appearance and react on each other to produce the coupled circuit curve shown. Finally when the ratio of optical to mechanical axes becomes larger a total of four resonant frequenices appear. Since a large number of crystals are used whose ratios of

optical to mechanical axes are greater than 0.2, it becomes a matter of some importance to investigate the causes of the additional resonances.

Interpretation of the Measured Resonance Frequency Curves of a Perpendicularly Cut Crystal

The plane wave assumption is valid for crystals whose width is less than 1/5 of their length, but it fails for wider crystals. It fails to represent a rectangular crystal because it does not allow for a wave motion in any other direction. That such a motion will occur is readily found by inspecting the stress-strain equations of a quartz crystal, given by equation (7).

$$\begin{aligned} -x_x &= s_{11}X_x + s_{12}Y_y + s_{13}Z_z + s_{14}Y_z, \\ -y_y &= s_{12}X_x + s_{11}Y_y + s_{13}Z_z - s_{14}Y_z, \\ -z_z &= s_{13}X_x + s_{13}Y_y + s_{33}Z_z, \\ -y_z &= s_{14}X_x - s_{14}Y_y + s_{44}Y_z, \\ -z_z &= s_{44}Z_x + s_{14}X_y, \\ -x_y &= s_{14}Z_x + \tfrac{1}{2}(s_{11} - s_{12})X_y, \end{aligned} \tag{7}$$

where x_x, y_y, z_z are the three components of extensional strain, and y_z, z_x, x_y the three components of shearing strains. X_x, Y_y, Z_z, Y_z, Z_x, and X_y are the applied stresses and s_{11}, etc. are the six elastic compliances of the crystal. Their values are not determined accurately but the best known values are given in equation (42). In this equation the X axis coincides with the electrical axis of the crystal, the Y axis with the mechanical axis, and the Z axis with the optical axis.

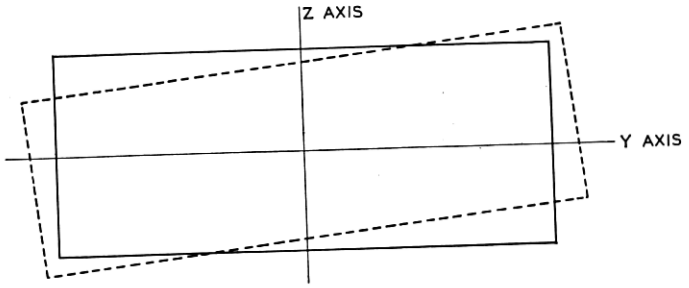

Fig. 26—Form of crystal distorted by an applied Y_y force.

Limiting ourselves now to an X or perpendicularly cut crystal the only stresses applied by the piezo-electric effect are an X_x, a Y_y, and a Y_z stress. Hence for such a crystal only four of the six possible types of motion are excited, three extensional motions x_x, y_y, z_z and one shear

motion y_z. Under static conditions, then, the motion at any point in the crystal is given as the sum of four elementary motions, three extensional motions and one shear motion. Moreover, these motions are coupled [13] as is shown by the fact that a force along one mode produces displacements in other modes of motion. Figure 26 shows how a perpendicularly cut crystal will be distorted for an applied Y_y force.

Suppose now that an alternating force is applied to the crystal. The simplest assumption that we can make regarding the motion is that the motion of any point is composed of four separate plane wave motions of the four types of vibration and that these react on each other in the way coupled vibrations are known to act in other mechanical [14] or electrical circuits. For the present purpose we can neglect motion along the X or electrical axis since this axis has been assumed small. The three remaining motions if existing alone will have resonances as shown by the solid lines of Fig. 27. That along the mechanical axis will have a constant frequency, since the mechanical axis is assumed constant, and is shown by the line C. The extensional motion along the optical axis will have a frequency inversely proportional to the length of the optical axis and will be represented by the line A of the figure. The shear vibration y_z, as shown by the section on the resonance frequency of a crystal vibrating in a shear mode, will have a frequency varying with dimension as shown by the line B.

In view of the coupling between the motions, the actual measured frequencies will be as shown by the dotted lines in agreement with well known coupled theory results.

If we compare these hypothetical curves with the actual measured values some degree of agreement is apparent. The main resonant frequency except in the region $0.2 < l_0/l_m < 0.3$ follows the dotted curve drawn. Also, the extensional motion along the optical axis has a frequency agreeing with that of Fig. 25. The shear vibration, however, has an entirely different curve from that conjectured. What is happen-

[13] The idea of elementary motions in the crystal being coupled together appears to have been first suggested in a paper by Lack "Observations on Modes of Vibration and Temperature Coefficients of Quartz Crystal Plates," *B. S. T. J.*, July, 1929, and was used by him to explain the effect of one mode of motion on the temperature coefficient of another mode and vice versa. The idea of associating this coupling with the elastic constants of the crystal occurred to the writer in 1930 but was not published at that time. It is, however, incorporated in a patent applied for some time ago on the advantages of crystals cut at certain orientations. More recently the same idea is given in a paper by E. Giebe and E. Bleckschmidt, *Annalen der Physik*, Oct. 16, 1933, Vol. 18, No. 4. They have extended their numerical calculations to include three modes of motion.

[14] This coupling is shown clearly for a mechanical system by one of the few rigorously solved cases of mechanical motion for two degrees of freedom—the vibration of a thin cylindrical shell—given by Love in "The Mathematical Theory of Elasticity," Fourth Edition, page 546.

ing there is I think evident from a consideration of Fig. 28. Here in solid lines are drawn two frequency curves one of which, B, is the shear frequency curve of Fig. 27. The other curve, D, has a rising frequency with an increase in the optical axis dimension. Assuming these vibra-

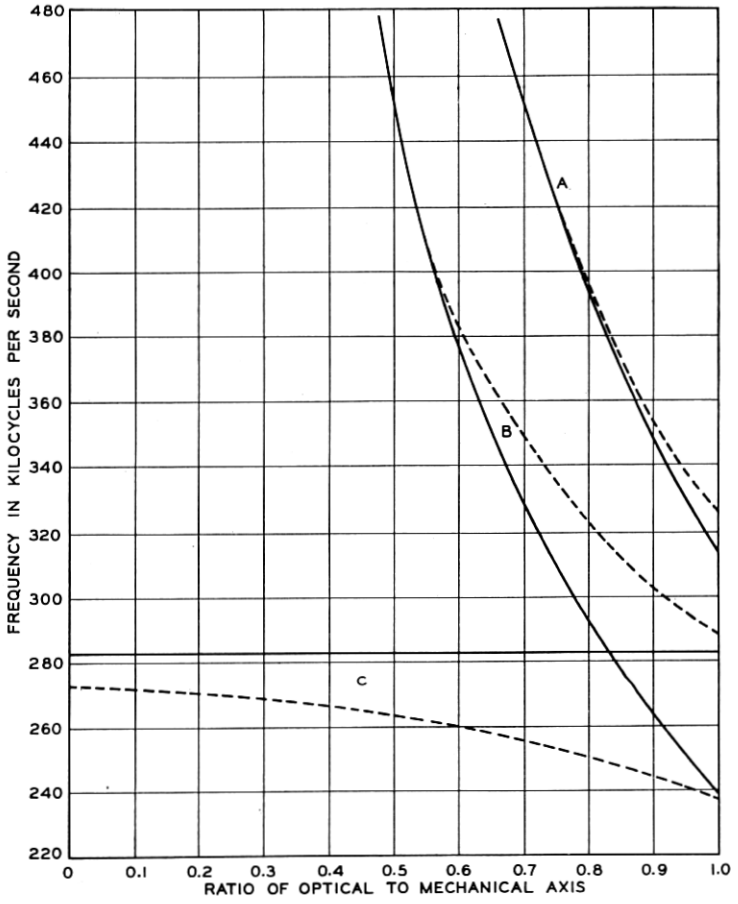

Fig. 27—Theoretical resonances of a perpendicularly cut crystal showing effect of coupling.

tions coupled a resonance frequency curve shown by the dotted line will be obtained. If this curve is substituted for the shear curve of Fig. 27 and the actual resonant frequency raised to take account of the effect of coupling with the longitudinal motion along the mechanical axis, a curve very similar to the measured curve of Fig. 25 is obtained.

The type of motion coupled to the shear motion is easily found. Its

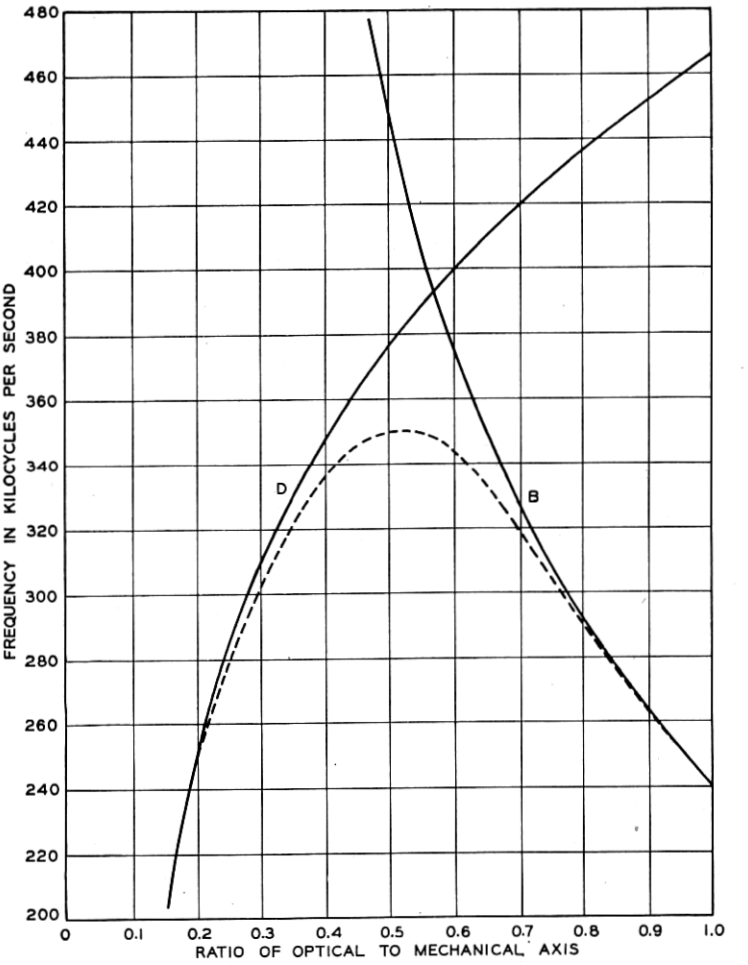

Fig. 28—Coupled frequency curve for shear and flexure vibrations.

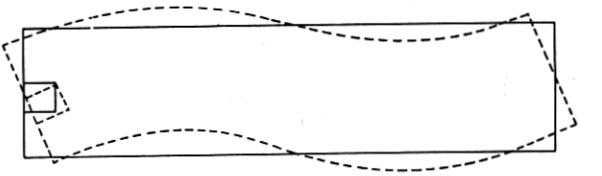

Fig. 29—Bar bent in its second flexural mode of vibration.

frequency increases as the optical axis dimension is increased and about the only type of motion which does this is a flexural motion as shown by Fig. 29. This figure shows the second type of motion possible to a bar in flexure rather than the first for experiments by Harrison [15] show that the frequency for the first type of motion is too low to account for this vibration. Harrison has also measured the frequencies of a bar in its second flexural mode and the solid line, D, of Fig. 28 is an actual plot of these measured frequencies up to a ratio of $l_0/l_m = 0.25$, which is as far as Harrison carries his measurements. The rest of the curve is obtained by extrapolation. There is no doubt then that a flexural motion is involved in this coupling. The mechanism by which the bar is driven in flexure will be evident if we observe what happens to a square on the crystal in the unstrained state. As shown by Fig. 29, its deformation is similar to that of a shear deformation. The amount of shear depends on the distance from the nodes of the crystal. Some of the shear is in one direction and some in the other but the two amounts are not balanced and hence a pure shear in one direction can excite a flexural motion of the crystal.

The strength of the coupling from the mechanical axis motion y_y to the shear motion y_z and the extensional motion along the optical axis z_z are indicated by the coupling compliances $s_{24}/\sqrt{s_{22}s_{44}}$ and $s_{23}/\sqrt{s_{22}s_{33}}$, respectively. From the values of these constants we find that the shear motion is more closely coupled than the z extensional motion, and this is indicated experimentally by the greater width of the shear line.

Effect of a Rotation of the Longest Axis with Respect to the Electrical Axis on the Resonances of a Crystal

From the qualitative explanation of the secondary resonances given above, it is possible to predict how these resonances will be affected by any change in the crystal which changes the constants determining the three modes of motion and their coupling coefficients. One method for varying these constants is to change the direction for cutting the crystal slab from the natural crystal. In the present paper consideration is limited to those crystals which have their major faces perpendicular to an electrical axis, i.e., a perpendicularly cut crystal with its longest direction rotated by an angle θ from the direction of the mechanical axis. The convention is adopted that a positive angle is a clockwise rotation of the principal axis for a right handed crystal, when the electrically positive face (determined by a squeeze) is up.

[15] "Piezo-Electric Resonance and Oscillatory Phenomena with Flexural Vibration in Quartz Plates," J. R. Harrison, *I. R. E.*, December, 1927.

For a left-handed crystal a positive angle is in a counter-clockwise direction.

In the section dealing with elastic and piezo-electric constants for rotated crystals (page 449) is given a method for determining the elastic constants of a rotated crystal and curves are given for the ten elastic constants. These have been worked out by Mr. R. A. Sykes of the Laboratories. The method of designation is the following: The X axis remains fixed and is designated by $1'$. The axis of greatest length is designated by $2'$, since in the unrotated crystal the mechanical axis, corresponding to the Y direction, is the axis of greatest length. Extensional motion perpendicular to the $2'$ axis is designanted by $3'$, and shear motion in the plane determined by the $2'$, $3'$ axes is designated by $4'$. The ten resulting constants s_{11}', s_{22}', s_{33}', s_{44}', s_{12}', s_{13}', s_{14}' s_{23}', s_{24}', s_{34}' are shown evaluated in terms of the angle θ on Fig. 30. Since

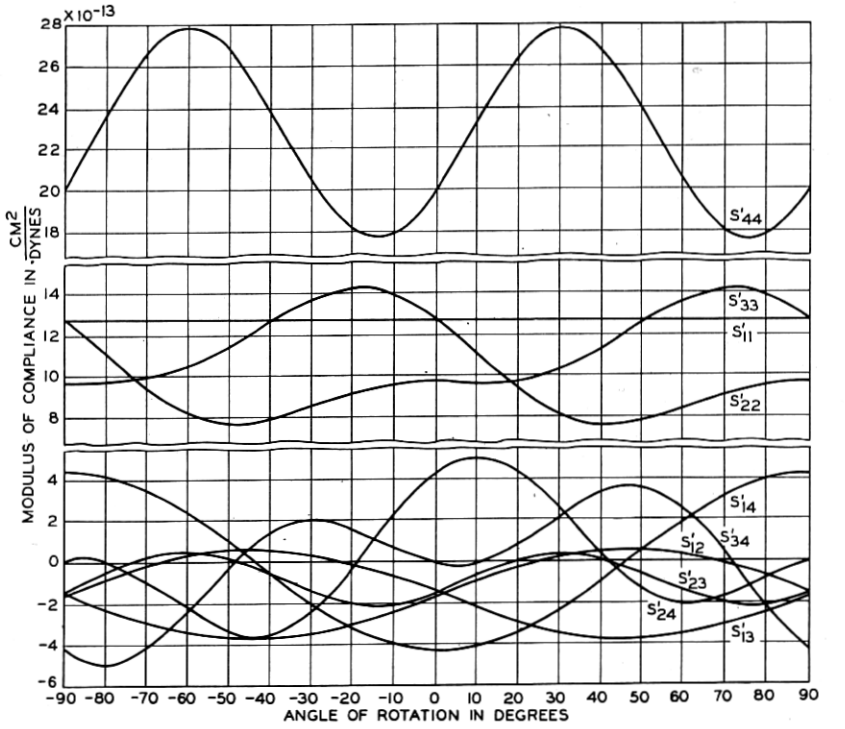

Fig. 30—Elastic compliances of a perpendicularly cut crystal as a function of the angle of rotation.

motion and coupling to motion along the X axis can be neglected, the constants of interest are s_{22}', s_{33}', s_{44}', s_{23}', s_{24}', s_{34}'. Since the $2'$ or y'

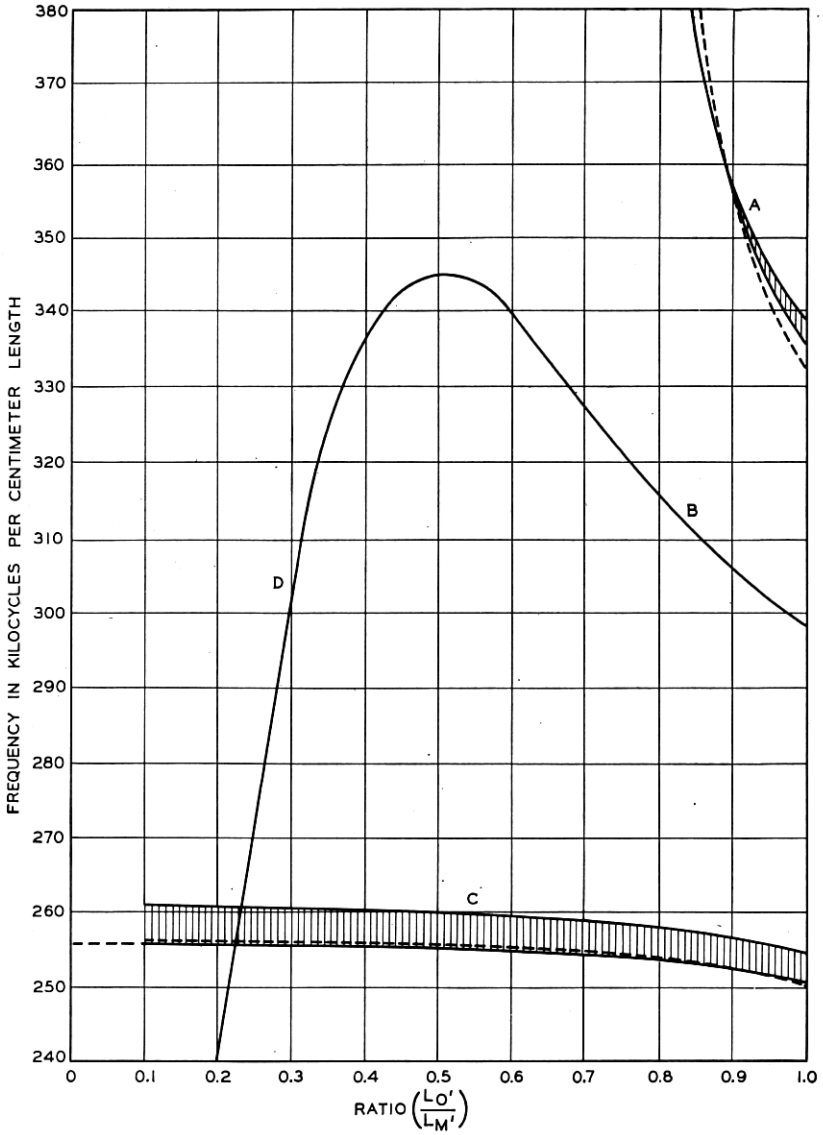

Fig. 31—Measured resonances of a $\theta = -18.5°$ perpendicularly cut crystal.

axis is the principal axis of motion, the mutual compliances of principal interest are s_{23}', determining the coupling between the Y' extensional motion and the Z' extensional motion, and s_{24}' determining the coupling between the Y' extensional motion and the Y_z' shear motion. It is the shear motion which is most objectionable, because it is more highly coupled than the Z' extensional motion, because it is lower in frequency, and because it is coupled to a flexural mode. Hence, if this motion can be eliminated or made very small, a much better crystal for most purposes is obtained. We note that if θ is $-18.5°$ or if $\theta = 41.5°$ the shear coupling coefficient vanishes and hence a force in the Y_y direction produces no y_z shear or vice versa. Of these the $-18.5°$ crystal is driven more strongly by the piezo-electric effect and hence has a more prominent resonance.

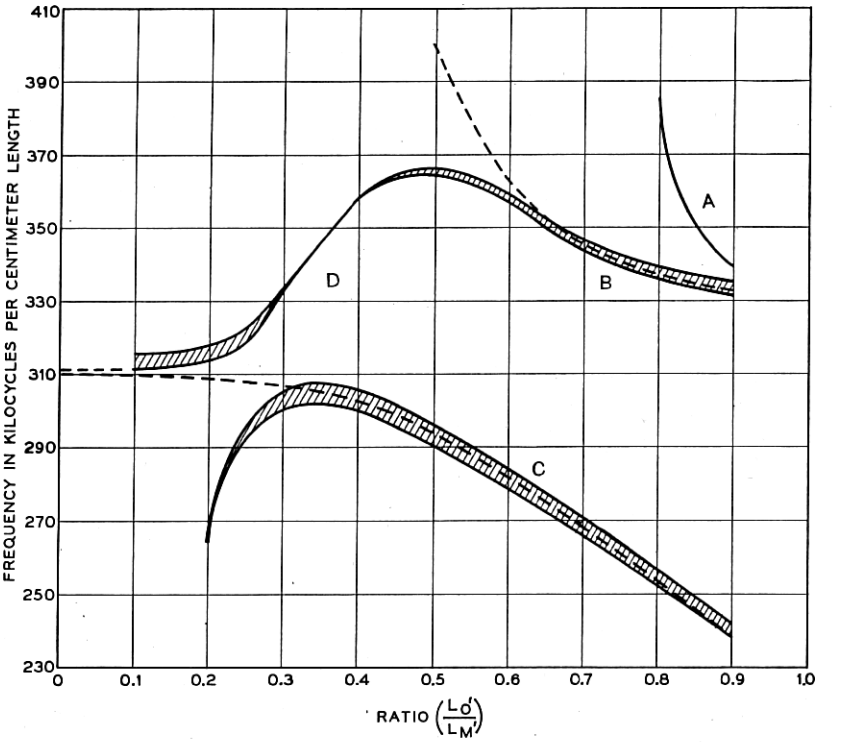

Fig. 32—Measured resonances of a $\theta = +18.5°$ perpendicularly cut crystal.

Accordingly the resonances of a $\theta = -18.5°$ cut crystal have been measured in a similar way to the $\theta = 0°$ cut crystal shown in Fig. 25. The result is shown on Fig. 31. As will be seen from the figure, the

shear resonance indicated by B is barely noticeable, while the z extensional mode indicated by A is somewhat stronger although higher in frequency. The frequency of the principal mode is not greatly affected by an increase in the z' axis until the ratio of axes is greater than .6. Another angle of some interest is $\theta = +18.5°$ since there the z' extensional coupling disappears. The resulting resonances are shown on Fig. 32. It will be noted that the z' extensional resonance curve A is very weak, while the shear curve B is quite pronounced.

An Equivalent Electrical Circuit for a Crystal Possessing Two Degrees of Motion

The above explanation accounts qualitatively for all the resonances observed in the crystal and how they are varied by a rotation of the crystal. It is desirable, however, to see if a quantitative check can be obtained from the known elastic constants of the crystal. To obtain a complete check would require a system capable of five degrees of motion. However, if we take the simplest case, the -18.5 degree cut crystal, only two modes of motion have to be considered, and even for the zero cut crystal, a good agreement is obtained by lumping the shear and extensional mode as one mode of motion and considering its reaction on the fundamental mode. Hence consideration is limited in this paper to a circuit having two modes of motion.

The properties of a single mode of motion can be represented for frequencies which do not exceed the first resonant frequency of the crystal, by the simple electrical circuit of Fig. 33A. Here the capaci-

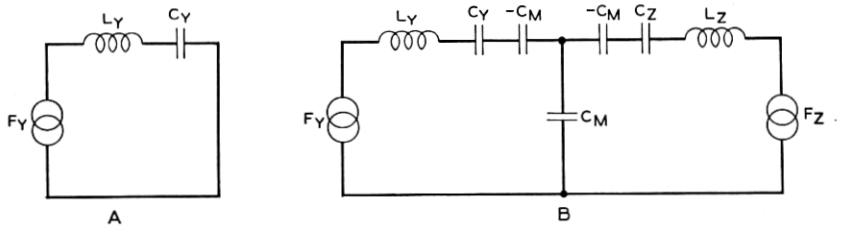

Fig. 33—Equivalent electrical circuit of a crystal having two modes of motion.

tance represents the mechanical compliance of the bar, the charge on the condenser represents a displacement per unit length of the bar, while the current flowing through the circuit represents the velocity of a point on the bar. The inductance represents the mass reaction of the crystal. The representation of the motion of a bar by a simple lumped circuit assumes that the bar moves as a whole, that is, if a force is applied to the body it contracts or expands equally at all parts of the

bar. This is contrary to actual conditions, since expansions or contractions proceed in the form of a wave from the ends of the bar toward the center. However, if consideration is limited to low frequencies, i.e. frequencies which do not exceed by much the first resonance of the bar, the approximation is good and a considerable simplification in the analysis is made. To take account of wave motion, the representation has to be an electric line as was pointed out in connection with acoustic filters.[16]

To represent two separate modes of motion and their coupling, the circuit shown by Fig. 33*B* is employed. A little consideration shows that the type of coupling existing in a crystal is capacitative since an extension along the mechanical axis produces a contraction along the optical axis, and vice versa. Since strains in mechanical terms are equivalent to charges in electrical terms, this type of coupling can be represented only by a capacitative network. This representation is entirely analogous to the T network representation for a transformer.[17] The constants of the network can be evaluated in terms of the elastic constants of the crystal as follows: For a -18.5 degree cut crystal, we can write the stress strain equation (7) as

$$\begin{aligned} y_y &= s_{22}' Y_y + s_{23}' Z_z, \\ z_z &= s_{23}' Y_y + s_{33}' Z_z, \end{aligned} \tag{8}$$

since we are neglecting motion along the X axis and since s_{24}', the coupling coefficient of the shear to the Y' axis is zero. No Y_z force is assumed acting. If we work out the equation for the charges on the condensers of the equivalent representation shown in Fig. 33*B* we have, with the charges and voltages directed as shown

$$\begin{aligned} Q_1 &= \frac{e_y C_y}{1 - K^2} + e_z \frac{\sqrt{C_y C_z} K}{1 - K^2}, \\ Q_2 &= \frac{e_y \sqrt{C_y C_z} K}{1 - K^2} + \frac{e_z C_z}{1 - K^2}, \end{aligned} \tag{9}$$

where K the coupling factor between the two modes of motion, is defined by the relation

$$K = \frac{\sqrt{C_y C_z}}{C_m}. \tag{10}$$

Associating Q_1 with y_y, the displacement per unit length, Q_2 with

[16] See "Regular Combination of Acoustic Elements," W. P. Mason, *B. S. T. J.*, April, 1927, p. 258.

[17] See, for example, p. 281 in the book "Transmission Circuits for Telephonic Communication" by K. S. Johnson.

z_z, e_y with Y_y and e_z with Z_z, we have on comparing (9) with (8)

$$s_{22}' = \frac{C_y}{1 - K^2}\,;\; s_{23}' = \frac{\sqrt{C_y C_z}K}{1 - K^2}\,;\; s_{33}' = \frac{C_z}{1 - K^2} \tag{11}$$

or inversely

$$C_y = s_{22}'\left[1 - \frac{s_{23}'^2}{s_{22}' s_{33}'}\right];\; C_z = s_{33}'\left[1 - \frac{s_{23}'^2}{s_{22}' s_{33}'}\right];\; K = \frac{s_{23}'}{\sqrt{s_{22}' s_{33}'}}. \tag{12}$$

If, now, alternating forces are applied to the crystal, another reaction to the applied force enters, namely the mass reaction of the crystal due to the inertia of the different parts. To take account of this reaction, the inductances are added to the two meshes representing mass reaction for the two modes of motion. To determine the value of the inductance, consider first the representation for one mode of motion shown by Fig. 33*A*. The resonant frequency of the system is given by

$$f_r = \frac{1}{2\pi\sqrt{LC}}. \tag{13}$$

On the other hand, the resonant frequency of a bar is given by

$$f_r = \frac{1}{2l\sqrt{\rho s}}, \tag{14}$$

where l is the length of the bar, s its compliance, and ρ its density. But in the above representation the capacitance C is the compliance constant s so that, on comparing (13) and (14) we find

$$L = \frac{l^2\rho}{\pi^2}. \tag{15}$$

In a similar manner for the coupled circuit, Fig. 33*B*, there results

$$L_y = \frac{l_y^2\rho}{\pi^2}\,;\; L_z = \frac{l_z^2\rho}{\pi^2}, \tag{16}$$

where l_y is the length of the crystal in centimeters along the y axis, and l_z the length of the crystal in centimeters along the z axis. Hence all of the constants of Fig. 33*B*, which represents the crystal for mechanical vibrations subject to the restrictions noted above, are determined and we should be able to predict all of the quantities which depend only on the mechanical constants of the crystal.

Of these the most important are the resonance frequencies of the crystal and their dependence on dimension, temperature coefficient and the like. To determine the natural mechanical resonance of a crystal,

we solve the network of Fig. 33*B* to find the frequencies of zero impedance for either an applied Y_y force or an applied Z_z force. The result is two frequencies f_1 and f_2 given by the coupled circuit equations

$$\begin{aligned} f_1^2 &= \tfrac{1}{2}[(f_A^2 + f_B^2) - \sqrt{(f_B^2 - f_A^2)^2 + 4K^2 f_A^2 f_B^2}], \\ f_2^2 &= \tfrac{1}{2}[(f_A^2 + f_B^2) + \sqrt{(f_B^2 - f_A^2)^2 + 4K^2 f_A^2 f_B^2}], \end{aligned} \tag{17}$$

where

$$f_A = \frac{1}{2\pi\sqrt{L_y C_y}} \text{ and } f_B = \frac{1}{2\pi\sqrt{L_z C_z}}. \tag{18}$$

Then f_A and f_B represent the natural frequencies along the Y and Z axis respectively when these two motions are not coupled together.

Two limiting cases of interest are obtainable from these relations. If f_B is much larger than f_A, the equations reduce to

$$\begin{aligned} f_1 &= f_A\sqrt{1 - K^2} = \frac{1}{2l_y\sqrt{\rho s_{22}'}}, \\ f_2 &= f_B = \frac{1}{2l_z\sqrt{\rho s_{33}'[1 - s_{23}'^2/s_{22}' s_{33}']}} \end{aligned} \tag{19}$$

upon substituting the value of the constants given before. The first equation shows that for a long thin rod the frequency depends on the elastic constant s_{22}', which is the inverse of Young's modulus. For the frequency f_2, which corresponds to that of a thin plate, a different elastic constant appears. Upon evaluating the expression $s_{33}'[1 - s_{23}'^2/s_{22}' s_{33}']$ in terms of the elastic constants which express the forces in terms of the strains—see equation (25)—we find that $s_{33}'(1 - s_{23}'^2/s_{22}' s_{33}') = 1/c_{33}$. c_{33} measures the ratio of force to strain when all the other coupling coefficients are set equal to zero, and corresponds to the frequency of one mode vibrating by itself without coupling to other modes. Hence the frequency of a thin plate should be

$$f = \frac{1}{2t}\sqrt{\frac{c_{nn}}{\rho}}, \tag{20}$$

where c_{nn} represents the elastic coefficient for the mode of motion considered, and t is the thickness of the plate. This deduction has been verified by experimental tests on thin plates.

Let us consider now the curves for the -18.5 degree cut crystal shown by Fig. 31. The values of the elastic constants for this case are

$$s_{22}' = 144 \times 10^{-14} \text{ cm.}^2/\text{dynes}; \; s_{23}' = -21.0 \times 10^{-14}; \; s_{33}' = 92.5 \times 10^{-14}. \tag{21}$$

Hence from equations (17), (18) and (21) one should be able to check the measured frequency curves of Fig. 31. The result is shown on the dotted lines of these curves. The agreement is quite good although a slightly better agreement would be obtained if s_{23} had a smaller value. Since these constants have never been measured with great accuracy, it is possible that they deviate somewhat from the curves of Fig. 30.

This theory can be applied also to a $\theta = +18.5$ degree cut crystal since the extensional coupling coefficient vanishes for this angle. The agreement is quite good if the frequency for the uncoupled mode given by the section on vibration in shear mode (page 446) is used in place of equation (14). The resonances for the $\theta = 0°$ cut crystal shown by Fig. 25 cannot be accounted for quantitatively by the simple theory given here since there are three modes of motion operating. The shear mode of motion is more closely coupled to the principal mode than is the Z_z extensional mode and hence a fair approximation is obtained by considering only the shear mode. However, for complete agreement the theory should be extended to a triply coupled circuit and that is not done in this paper.

Another phenomenon of interest which can be accounted for by the circuit of Fig. 33*B* is the temperature coefficient of the crystal and its variation with different ratios of axes and different angles of rotation. To obtain the relation, we assume that each of the vibrations may have a temperature coefficient of its own as may also the coefficient of coupling K. If a small change of temperature occurs, f_1 will change to $f_1(1 + T\Delta T)$, f_A to $f_A(1 + T_A\Delta T)$, f_B to $f_B(1 + T_B\Delta T)$ and K to $K(1 + T_K\Delta T)$. Assuming ΔT small so that its squares and higher powers can be neglected, we find from equation (17) that

$$T = \frac{1}{2f_1^2}\left[T_A f_A^2 \left[1 + \frac{f_B^2(1 - 2K^2) - f_A^2}{\sqrt{(f_B^2 - f_A^2)^2 + 4K^2 f_A^2 f_B^2}} \right] + T_B f_B^2 \right.$$
$$\times \left[1 - \frac{f_B^2(1 + 2K^2) - f_A^2}{\sqrt{(f_B^2 - f_A^2)^2 + 4K^2 f_A^2 f_B^2}} \right]$$
$$\left. - \frac{2T_K f_A^2 f_B^2}{\sqrt{(f_B^2 - f_A^2)^2 + 4K^2 f_A^2 f_B^2}} \right]. \quad (22)$$

The temperature coefficients of the six elastic constants have been measured at the Laboratories [18] by measuring the frequency temperature coefficients of variously oriented crystals. The temperature coefficients of the six elastic constants can be calculated from these

[18] These coefficients have been evaluated in cooperation with Messrs. F. R. Lack, G. W. Willard and I. E. Fair and their work is discussed in detail in their companion paper in this issue of the *B. S. T. J.*

measurements and have been found to be, in parts per million per degree centigrade:

$$T_{s_{11}} = +13;\ T_{s_{12}} = -1230;\ T_{s_{13}} = -347; \qquad (23)$$
$$T_{s_{14}} = +130;\ T_{s_{33}} = +213;\ T_{s_{44}} = +172.$$

Using these values and neglecting the extensional motion Z_z, the temperature coefficients calculated from equation (22) for a 0 degree cut crystal are shown on the dotted line of Fig. 5 and agree quite well with the measured values.

The Resonance Frequencies of a Crystal Vibrating in a Shear Mode

The equations of motion for any aelotropic body are

$$\rho\frac{\partial^2 u}{\partial t^2} = \frac{\partial X_x}{\partial x} + \frac{\partial X_y}{\partial y} + \frac{\partial X_z}{\partial z},$$
$$\rho\frac{\partial^2 v}{\partial t^2} = \frac{\partial Y_x}{\partial x} + \frac{\partial Y_y}{\partial y} + \frac{\partial Y_z}{\partial z}, \qquad (24)$$
$$\rho\frac{\partial^2 w}{\partial t^2} = \frac{\partial Z_x}{\partial x} + \frac{\partial Z_y}{\partial y} + \frac{\partial Z_z}{\partial z},$$

where u, v, w are the displacements of any point in the crystal along the x, y, z axes respectively and X_x, etc. are the six applied stresses. The strains have been expressed in terms of the stresses by equation (7). It is more advantageous for the present purpose to express the stresses in terms of the strains, which can be done by the following equations:

$$X_x = c_{11}x_x + c_{12}y_y + c_{13}z_z + c_{14}y_z,$$
$$Y_y = c_{12}x_x + c_{22}y_y + c_{23}z_z + c_{24}y_z,$$
$$Z_z = c_{13}x_x + c_{23}y_y + c_{33}z_z, \qquad (25)$$
$$Y_z = c_{14}x_x + c_{24}y_y + c_{44}y_z,$$
$$Z_x = c_{44}z_x + c_{14}x_y,$$
$$X_y = c_{14}z_x + \tfrac{1}{2}(c_{11} - c_{12})x_y,$$

where the c's are the elastic constants and the strains x_x, etc., are given in terms of the displacements u, v, w by the equations

$$x_x = \frac{\partial u}{\partial x};\ y_y = \frac{\partial v}{\partial y};\ z_z = \frac{\partial w}{\partial z};\ y_z = \left(\frac{\partial v}{\partial z} + \frac{\partial w}{\partial y}\right);$$
$$z_x = \left(\frac{\partial w}{\partial x} + \frac{\partial u}{\partial z}\right);\ x_y = \left(\frac{\partial u}{\partial y} + \frac{\partial v}{\partial x}\right). \qquad (26)$$

In equation (24) there exist the reciprocal relations

$$X_y = Y_x;\ X_z = Z_x;\ Y_z = Z_y. \qquad (27)$$

For a free edge, i.e. no resulting forces being applied to the crystal, the conditions existing for every point of the boundaries are

$$\begin{aligned} X_\nu &= X_x \cos(\nu,x) + X_y \cos(\nu,y) + X_z \cos(\nu,z) = 0, \\ Y_\nu &= Y_x \cos(\nu,x) + Y_y \cos(\nu,y) + Y_z \cos(\nu,z) = 0, \\ Z_\nu &= Z_x \cos(\nu,x) + Z_y \cos(\nu,y) + Z_z \cos(\nu,z) = 0, \end{aligned} \tag{28}$$

where ν is the normal to the boundary under consideration.

If these equations are combined and completely solved, the motion of a quartz crystal is completely determined. The results which were obtained above in an approximate manner could be rigorously solved. However, on account of the difficulty [19] of the solution, this is not attempted here. In the present section it is simply the purpose to find out what resonances a crystal will have if it is vibrating in a shear mode only. To avoid setting up motion in the other modes of vibration, the coupling elasticities c_{14}, c_{24}, c_{34} are assumed zero. Similarly if c_{12}, c_{13}, c_{23} were set equal to zero we should have the possibility of three extensional modes and one shear mode vibrating simultaneously with no reaction on one another, and the equation of motion would be

$$\begin{aligned} \rho \frac{\partial^2 u}{\partial t^2} &= \frac{\partial}{\partial x}(c_{11}x_x), \\ \rho \frac{\partial^2 v}{\partial t^2} &= \frac{\partial}{\partial y}(c_{22}y_y) + \frac{\partial}{\partial_z}[c_{44}y_z], \\ \rho \frac{\partial^2 w}{\partial t^2} &= \frac{\partial}{\partial y}(c_{44}y_z) + \frac{\partial}{\partial z}[c_{33}z_z]. \end{aligned} \tag{29}$$

The displacements u, v, and w would be the sum of the displacements caused by the four motions. To find the displacements and resonances caused by the shear mode y_z, we neglect the other modes and have the equations

$$\begin{aligned} \rho \frac{\partial^2 v}{\partial t^2} &= c_{44} \frac{\partial}{\partial z}(y_z), \\ \rho \frac{\partial^2 w}{\partial t^2} &= c_{44} \frac{\partial}{\partial y}(y_z). \end{aligned} \tag{30}$$

Differentiating the first of equations (30) by $\frac{\partial}{\partial z}$, and the second by $\frac{\partial}{\partial y}$, and adding, there results,

$$\rho \frac{\partial^2}{\partial t^2}\left(\frac{\partial v}{\partial z} + \frac{\partial w}{\partial y}\right) = c_{44}\left[\frac{\partial^2 y_2}{\partial y^2} + \frac{\partial^2 y_2}{\partial z^2}\right]. \tag{31}$$

[19] For example if motion is limited to the y and z directions, and the coefficient c_{14} is set equal to zero, the equations reduce approximately to those for a plate bent in flexure, and this case has never been solved for the boundary condition of interest here, namely all four edges being free to move—see Rayleigh "Theory of Sound," page 372, Vol. I, 1923 edition.

Since $\frac{\partial v}{\partial z} + \frac{\partial w}{\partial y} = y_z$, this reduces to

$$\frac{\partial^2 y_z}{\partial t^2} = c^2 \left[\frac{\partial^2 y_z}{\partial y^2} + \frac{\partial^2 y_z}{\partial z^2} \right], \tag{32}$$

where $c^2 = c_{44}/\rho$.

For a simple harmonic vibration, of frequency f, the equation reduces to

$$\left[\frac{\partial^2 y_z}{\partial y^2} + \frac{\partial^2 y_z}{\partial z^2} \right] + \frac{p^2}{c^2} y_z = 0, \tag{33}$$

where $p = 2\pi f$. The solution of this equation consistent with the boundary conditions (28) is

$$y_z = \Sigma\Sigma A_{mn} \left[\sin \frac{m\pi y}{a} \sin \frac{n\pi z}{b} \right] \cos pt, \tag{34}$$

where a is the length of the crystal in the y direction, b the length of the crystal in the z direction, and m and n are integers. Substituting this equation in the equation (32), we find that it is a solution provided

$$\left[\frac{m^2\pi^2}{a^2} + \frac{n^2\pi^2}{b^2} \right] = \frac{p^2}{c^2} = \frac{(2\pi f)^2}{c^2}. \tag{35}$$

Hence the resonant frequencies of the crystal in shear vibration are

$$f = \frac{c}{2} \sqrt{\frac{m^2}{a^2} + \frac{n^2}{b^2}}. \tag{36}$$

To find the shape of the deformed crystal, we have from (30) for simple harmonic vibration

$$v = -\frac{c^2}{p^2} \frac{\partial y_z}{\partial z} = \frac{-a^2b^2}{m^2\pi^2b^2 + n^2\pi^2a^2} \frac{\partial y_z}{\partial z}, \tag{37}$$

$$w = -\frac{c^2}{p^2} \frac{\partial y_z}{\partial y} = \frac{-a^2b^2}{m^2\pi^2b^2 + n^2\pi^2a^2} \frac{\partial y_z}{\partial y}. \tag{38}$$

The cases $m = 0$, $n = 1$ and $m = 1$, $n = 0$ require a stress known as a simple shear to excite them, whereas the stress applied by the piezo-electric effect is a pure shear. Hence the case $m = 1$, $n = 1$ provides the lowest frequency solution. The displacements v and w for this case are by equations (34), (37) and (38)

$$\begin{aligned} v &= \frac{-a^2b\pi}{\pi^2a^2 + \pi^2b^2} \left(\sin \frac{\pi y}{a} \cos \frac{\pi z}{b} \right); \\ w &= -\frac{ab^2\pi}{\pi^2a^2 + \pi^2b^2} \left(\cos \frac{\pi y}{a} \sin \frac{\pi z}{b} \right). \end{aligned} \tag{39}$$

The resulting distortion of the crystal is shown by Fig. 34.

We can conclude, therefore, that the solution for a shear vibration in a quartz crystal will be given by equation (34). It is obvious from Fig. 34 that the shear vibration will have a strong coupling to a bar

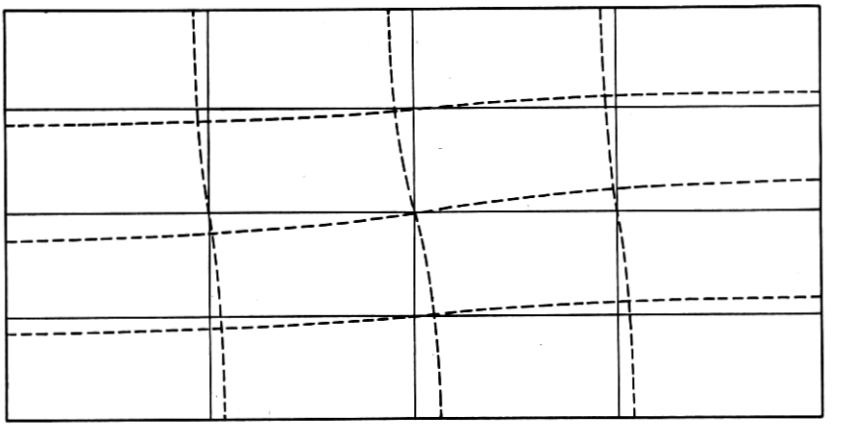

Fig. 34—Form of crystal in shear vibration.

bent in its second mode of flexure, since the form of the bent bar, as shown by Fig. 29, is very closely the same as a given displacement line in the crystal vibrating in shear. Little coupling should exist between the shear mode and a bar in its first flexure mode, since this mode of flexure requires a displacement which is symmetrical on both sides of the central line whereas the bar vibrating in shear has a motion in which the displacement on one side of the center line is the opposite of the displacement on the other side of the center line.

The Elastic and Piezo-Electric Constants of Quartz for Rotated Crystals [20]

W. Voigt [21] gives for the stress strain and piezo-electric relation in a quartz crystal, for the three extensions and one shear found above,

$$\begin{aligned} -x_x &= s_{11}X_x + s_{12}Y_y + s_{13}Z_z + s_{14}Y_z, \\ -y_y &= s_{12}X_x + s_{22}Y_y + s_{23}Z_z + s_{24}Y_z, \\ -z_z &= s_{13}X_x + s_{23}Y_y + s_{33}Z_z + s_{34}Y_z, \\ -y_z &= s_{14}X_x + s_{24}Y_y + s_{34}Z_z + s_{44}Y_z, \end{aligned} \tag{40}$$

$$-P_x = d_{11}X_x + d_{12}Y_y + d_{13}Z_z + d_{14}Y_z, \tag{41}$$

[20] The material of this section was first derived by Mr. R. A. Sykes of the Bell Telephone Laboratories.

[21] W. Voigt, Lehrbach Der Kristallphysik.

where

x_x, y_y, z_z = extensional strains = elongation per unit length,
X_x, Y_y, Z_z = extensional stresses = force per unit area,
y_z = shearing strain = cos of an angle,
Y_z = shearing stress = force per unit area,
s_{ij} = elastic compliances = displacement per dyne,
d_{ij} = piezo-electric constants = e.s.u. charge per dyne,
P_x = piezo-electric polarization = charge per unit area.

The best measured values for these constants when the X axis coincides with the electric axis of the crystal, the Y axis with the mechanical axis and the Z axis with the optical axis, are

$$\begin{aligned}
s_{11} &= s_{22} = 127.2 \times 10^{-14} \text{ cm.}^2/\text{dyne}, \\
s_{12} &= -16.6 \times 10^{-14} \text{ cm.}^2/\text{dyne}, \\
s_{13} &= s_{23} = -15.2 \times 10^{-14} \text{ cm.}^2/\text{dyne}, \\
s_{24} &= -s_{14} = 43.1 \times 10^{-14} \text{ cm.}^2/\text{dyne}, \\
s_{33} &= 97.2 \times 10^{-14} \text{ cm.}^2/\text{dyne}, \\
s_{34} &= 0, \\
s_{44} &= 200.5 \times 10^{-14} \text{ cm.}^2/\text{dyne}, \\
d_{11} &= -d_{12} = -6.36 \times 10^{-8} \frac{\text{e.s.u. charge}}{\text{dyne}}, \\
d_{13} &= 0 \\
d_{14} &= 1.69 \times 10^{-8} \frac{\text{e.s.u. charge}}{\text{dyne}}.
\end{aligned} \tag{42}$$

If, now, we maintain the direction of the electrical axis but rotate the direction of the principal axis by some angle θ, the resulting constants of equations (40) and (41) undergo a change.

Let the direction cosines for the new axes be given by

	x	y	z
x'	l_1	m_1	n_1
y'	l_2	m_2	n_2
z'	l_3	m_3	n_3

(43)

The convention is adopted that a positive angle θ is a clockwise rotation of the principal axis of the crystal, when the electrically positive face (determined by a squeeze) is up. For a left-handed crystal a positive angle is in a counter clockwise direction. θ is the angle between the previously unprimed and the primed axes.

If we transform only the y and z axes, there results

$$\begin{aligned} l_2 &= l_3 = m_1 = n_1 = 0, \\ l_1 &= 1, \\ m_2 &= n_3 = \cos\theta, \\ -n_2 &= m_3 = \sin\theta. \end{aligned} \tag{44}$$

Love [22] gives the transformation for the stress and the strain functions as

$$\begin{aligned} x_x' &= x_x l_1^2 + y_y m_1^2 + z_z n_1^2 + y_z m_1 n_1, \\ y_y' &= x_x l_2^2 + y_y m_2^2 + z_z n_2^2 + y_z m_2 n_2, \\ z_x' &= x_x l_3^2 + y_y m_3^2 + z_z n_3^2 + y_z m_3 n_3, \\ y_z' &= 2x_x l_2 l_3 + 2y_y m_2 m_3 + 2z_z n_2 n_3 + y_z(m_2 n_3 + m_3 n_2), \end{aligned} \tag{45}$$

$$\begin{aligned} X_x' &= X_x l_1^2 + Y_y m_1^2 + Z_z n_1^2 + Y_z 2m_1 n_1, \\ Y_y' &= X_x l_2^2 + Y_y m_2^2 + Z_z n_2^2 + Y_z 2m_2 n_2, \\ Z_x' &= X_x l_3^2 + Y_y m_3^2 + Z_z n_3^2 + Y_z 2m_3 n_3, \\ Y_z' &= X_x l_2 l_3 + Y_y m_2 m_3 + Z_z n_2 n_3 + Y_z(m_2 n_3 + m_3 n_2). \end{aligned} \tag{46}$$

Substituting (44) in (45) and (46) and then expressing x_x, y_y . . . X_x, Y_y . . ., etc., in terms of x_x', y_y' . . . X_x', Y_y' . . ., etc., we may substitute these values in equations (40) and (41) to give the stress-strain and polarization in a crystal whose rectangular axes do not coincide with the real optical and mechanical axis. Performing the above operations, a new set of constants s_{ij}', are obtained which are functions of θ, namely:

$$s_{11}' = s_{11},$$

$$s_{12}' = \tfrac{1}{2}[s_{12} + s_{13} + (s_{12} - s_{13})\cos 2\theta - s_{14}\sin 2\theta],$$

$$s_{13}' = \tfrac{1}{2}[s_{13} + s_{12} + (s_{13} - s_{12})\cos 2\theta + s_{14}\sin 2\theta],$$

$$s_{14}' = s_{14}\cos 2\theta + (s_{12} - s_{13})\sin 2\theta,$$

$$s_{22}' = s_{11}\cos^4\theta + s_{33}\sin^4\theta + 2s_{14}\cos^3\theta\sin\theta + (2s_{13} + s_{44})\sin^2\theta\cos^2\theta,$$

$$s_{23}' = s_{13}(\cos^4\theta + \sin^4\theta) + s_{14}(\sin^3\theta\cos\theta - \cos^3\theta\sin\theta) + (s_{11} + s_{33} - s_{44})\sin^2\theta\cos^2\theta,$$

$$s_{24}' = -s_{14}(\cos^4\theta - 3\sin^2\theta\cos^2\theta) + (2s_{11} - 2s_{13} - s_{44})\cos^3\theta\sin\theta + (2s_{13} - 2s_{33} + s_{44})\sin^3\theta\cos\theta,$$

$$s_{33}' = s_{33}\cos^4\theta + s_{11}\sin^4\theta - 2s_{14}\sin^3\theta\cos\theta + (2s_{13} + s_{44})\sin^2\theta\cos^2\theta,$$

[22] "The Mathematical Theory of Elasticity," Cambridge University Press, pp. 42 and 78.

$$s_{34}' = s_{14}(\sin^4\theta - 3\sin^2\theta\cos^2\theta) + (2s_{11} - 2s_{13} - s_{44})\sin^3\theta\cos\theta + (2s_{13} - 2s_{33} + s_{44})\cos^3\theta\sin\theta,$$

$$s_{44}' = (4s_{33} + 4s_{11} - 8s_{13} - 2s_{44})\sin^2\theta\cos^2\theta + 4s_{14} \times (\sin^3\theta\cos\theta - \sin\theta\cos^3\theta) + s_{44}(\sin^4\theta + \cos^4\theta)$$

and

$$d_{11}' = d_{11},$$
$$d_{12}' = -\tfrac{1}{2}[d_{11}(1 + \cos 2\theta) + d_{14}\sin 2\theta],$$
$$d_{13}' = -\tfrac{1}{2}[d_{11}(1 - \cos 2\theta) - d_{14}\sin 2\theta],$$
$$d_{14}' = d_{14}\cos 2\theta - d_{11}\sin 2\theta.$$

The curves representing the s' values for varying angles of orientation are plotted on Fig. 30 while the values of d' are plotted on Fig. 35.

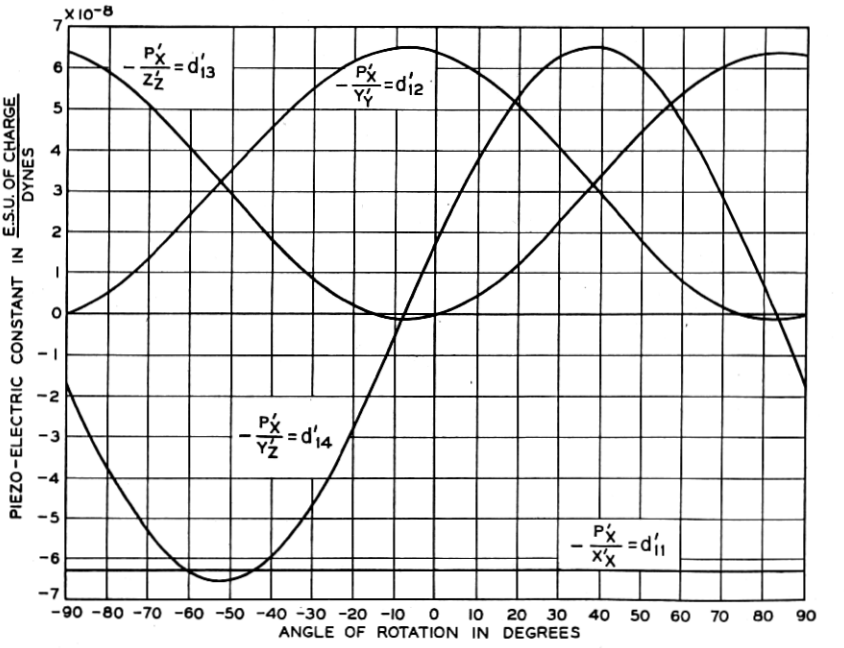

Fig. 35—Piezo-electric constants of a perpendicularly cut crystal as a function of the angle of rotation.